12-17-2010

Pattern Recognition of Power Systems Voltage Stability Using Real Time Simulations

Nagendrakumar Beeravolu
University of New Orleans

Pattern Recognition of Power Systems Voltage Stability Using Real Time Simulations

A Thesis

Submitted to Graduate Faculty of the
University of New Orleans
in partial fulfillment of the
requirements for the degree of

Master of Science
In
Engineering
Electrical

By

Nagendrakumar Beeravolu

B. Tech. JNTU, 2007

December, 2010

Acknowledgements

This thesis would not have been possible without the guidance and the help of several individuals who in one way or another contributed and extended their valuable assistance in the preparation and completion of this study.

First I wish to express my utmost gratitude to my advisor Prof. Dr. Parviz Rastgoufard who was abundantly helpful and offered invaluable assistance, support and guidance to finish this thesis. My association with him for over two years was a rewarding experience. Deepest gratitude to the members of the supervisory committee, Assis. Prof. Dr. Ittiphong Leevongwat and Prof. Dr. Edit Bourgeois for their great support throughout my masters to finish this study. I would like to thank Entergy-UNO Power and Research Laboratory for providing appropriate tools to finish this task.

I would specially like to thank Dr. Sze Mei Wong, without her knowledge and assistance this study would not have been successful.

Last, I would like to acknowledge and thank my parents, my sister and all of my friends for their encouragement and moral support to finish this task.

Table of Contents

List of Tables

List of Figures

Abstract

The basic idea deals with detecting the voltage collapse ahead of time to provide the operators a lead time for remedial actions and for possible prevention of blackouts. To detect cases of voltage collapse, we shall create methods using pattern recognition in conjunction with real time simulation of case studies and shall develop heuristic methods for separating voltage stable cases from voltage unstable cases that result in response to system contingencies and faults. Using Real Time Simulator in Entergy-UNO Power & Energy Research Laboratory, we shall simulate several contingencies on IEEE 39-Bus Test System and compile the results in two categories of stable and unstable voltage cases. The second stage of the proposed work mainly deals with the study of different patterns of voltage using artificial neural networks. The final stage deals with the training of the controllers in order to detect stability of power system in advance.

KEY WORDS: Real time simulator, Voltage stability, Voltage collapse, Blackout, Pattern recognition, Hypersim, EMTP

Chapter 1

Introduction

1.1 A Review of Voltage Stability

Security of power systems operation is gaining ever increasing importance as the system operates closer to its thermal and stability limits. Power system stability- the most important index in power system operation- may be categorized under two general classes relating to the magnitude and to the angle of bus voltages. Voltage stability focuses on determining the proximity of bus voltage magnitudes to pre determined and acceptable voltage magnitudes and angle stability focuses on the investigation of voltage angles as the balance between supply and demand changes due to occurrence of faults or disturbances in the system. Voltage stability is slowly varying phenomena while angle stability is relatively faster and deals with systems dynamics described mathematically by differential equations of generators in the system.

Voltage instability of a power system is its inability to maintain the steady state voltage after a disturbance in the system. The possible outcomes of voltage instability are loss of load in an area where the voltage values are relatively smaller than the voltage in other areas of the system, and hence, a candidate for load shedding in the areas with smaller voltage magnitudes. The Main factor contributing to voltage instability in an area is an increase in voltage drop when the active and reactive power flow through the transmission line is more compared to initial conditions. There is another possibility that increase in rotor angles of machines will also cause more voltage drop in turn which will lead to voltage instability.

Voltage instability or voltage collapse in a power system while is normally perceived as a slowly varying phenomena, it could be caused by system dynamics. The mechanism leading to voltage collapse normally starts from lowering of voltage at an area due to the areas increase in load demand and hence changing the system steady state conditions slowly requiring the stabilizing elements such as load tap changers, voltage regulators, and static and dynamic compensators to respond to the system changes and the new system conditions. If these elements while stabilizing the system exceed their operating limits, they will be removed from system operation, and hence drive the system to a more severe operating condition and closer to the point of voltage collapse and eventually to operating conditions that are uncontrollable. Because of interaction of these components and due to different dynamic time response of these equipments, voltage collapse will take fraction of seconds to tens of minutes. Due to variation in time responses, appropriate mathematical models encompassing steady state to models that capture dynamics in almost real-time may be required to predict proximity and occurrence of voltage collapse in real-size power systems.

Main reason for the voltage collapse is when the transmission lines are operating very close to their thermal limits and forced to transmit more power over a long distance or when the power system has insufficient reactive power for transmission to the area with increasing load. In large scale systems voltage collapse include voltage magnitude and voltage angle under heavy loading conditions. In some situations it is hard to decouple the angle and magnitude instability from each other.

Two types of system analysis are possible; static system and dynamic system analysis and using each approach is appropriate for specific system conditions and each bear its own advantage and disadvantage which we shall address in this research. Design and analysis of

accurate methods to evaluate the voltage stability of a power system and predicting incipient voltage instabilities are therefore of special interest in the field of power systems. Dynamic analyses provide the most accurate indication of the time response of the system and are useful for predicting fast occurring voltage collapses in the system but these will not provide much information about sensitivity or degree of stability. On the other hand static analyses that are based on performing system-wide sensitivity will provide the information necessary for concluding degree of instability. Static analysis involves computation of algebraic rather than solution of differential equations, and hence, much faster compared to dynamic analysis for both on-line and off-line studies. But static analysis cannot investigate the dynamic reasons for voltage instability that may be embedded in the energy content of the system only a few seconds after occurrence of a system disturbance and long before the ultimate result of system voltage collapse. We shall outline our approach in using static and dynamic system models for prediction of patterns that may be detectible a few seconds after disturbances in predicting system voltage instabilities later in this chapter.

1.2 Review of Static Analysis Methods of Voltage Stability:

There are many research publications ranging from papers to books on use of static analysis of voltage stability. Most of these publications document approaches that are based on using system's Jacobian matrix and use of the Jacobian matrix in identifying its singularities. The singularities of the Jacobian matrix provide a guide to the point of system voltage collapse. Static approaches capture snapshots of system conditions at various time frames and can determine the overall stability of the system or proximity and margin to unstable at that particular time frame [1]. A variety of tools like multiple load flow solutions [2], load flow feasibility [3], optimal power flow [4], steady state stability [5], modal analysis [6,7,8-11], the P-

V curve, Q-V curve, Eigen value, singular value of Jacobian matrix [12,13], sensitivity and energy based methods have been proposed [1,14-19] on static analysis of voltage stability.

In the past all the utilities depended on conventional power flow programs for static analysis and the voltage stability was determined by computing P-V and V-Q curves at different buses in the system while the load at these buses were increased. This type of static analysis is a time consuming process because it has to undergo a large number of power flow solutions-several studies for each bus in the system. Also, these curves will not provide much information about cause of instability and the procedures are mainly concentrated on individual buses in the power system network. There are some approaches like V-Q sensitivity modal analysis which provide more information regarding voltage stability when compared to P-V and V-Q curves [1].

V-Q sensitivity analysis [1] which is used in modal analysis is a good measure for sensitivity of a system. This will use the same conventional power flow model which has a system Jacobian matrix. Generally system voltage stability is affected by P and Q, but for V-Q sensitivity analysis, P is kept constant and the voltage stability is determined by considering incremental relationship between Q and V. When P is kept constant the Jacobian matrix reduces to reduced Jacobian matrix and inverse of this matrix is the reduced V-Q Jacobian matrix where the i^{th} diagonal element of the matrix is the V-Q sensitivity of the i^{th} bus. A positive V-Q sensitivity represents a stable operation, smaller value of sensitivity implies more stable system and as the sensitivity value increases stability decreases. A negative value for V-Q sensitivity represents unstable operation.

J. Bian [20] compared various methods for studying voltage stability and proposed [47] to use the smallest Eigen values λ_{min} of the Jacobian matrix to measure voltage stability level of a

system. The smallest Eigen value is defined as the voltage stability margin and the singularity of the Jacobian matrix, reflected by $\lambda_{min}=0$, serves as the voltage instability indicator.

G.K. Morison, B. Gao, P. Kundar proposed a method referred to V-Q modal analysis [11] in 1992. This method is based on using the reduced Jacobian matrix formed in V-Q sensitivity analysis and it will provide proximity of the system to voltage instability as well as the main contributing factor for it. In this method smaller number of Eigen values are calculated from the reduced Jacobian matrix which keeps the Q-V relationship of the network and also includes the characteristics of generators, loads, reactive power compensating devices, and HVDC converters. The Eigen values of reduced Jacobian matrix will identify different modes of the system which will lead to voltage unstability. The magnitude of the Eigen value provides a relative measure of proximity to voltage instability. If the magnitude of modal Eigen value is equal to zero then the corresponding modal voltage collapses. Left and right Eigen vectors of critical modes will provide the information concerning the mechanism for the voltage collapse by identifying the elements that participate in the ultimate voltage collapse in the system. For this purpose they propose a concept called bus participation factor. Branches with large participation factors to the critical mode will consume more reactive power for incremental change in reactive power and will lead to the voltage instability [11]. S. Chandrabhan and G. Marcus have developed a PC-based MATLAB prototype application [21] to analyze the voltage stability of a power network using modal analysis proposed in [11] and some additional techniques like power flow analysis, V-P/V-Q curves.

Modal analysis has some disadvantages [22] in requiring the Jacobian matrix to be a square matrix, suitable for analyzing only PQ bus reactive power control where the active power is considered as zero, and assuming constant voltages by not considering generator AVR at PV

buses. C. Li-jun and E. Istavan [22] present their work by considering static voltage stability analysis by use of singular value approach for both active and reactive power control. They applied the voltage magnitude of critical buses as output and feasible controls as input signals and developed a MIMO (multi input and multi output) transfer function of multi machine system and singular value decomposition (SVD) to identify the maximum and minimum singular values of the transfer function matrix . The authors propose to monitor the maximum input vector and the maximum output vector and to correspond the change to the input that has the largest influence on the corresponding output and the buses where the voltage magnitude is critical.

Static analysis for voltage stability methods are easier to implement because modeling of loads and generators are simple and requires less computing time in the simulation. But on the other hand it is not accurate because of the models considered for loads and generators.

1.3 Review of Dynamic Analysis Methods of Voltage Stability:

Power system is a typical large dynamic system and its dynamic behavior has great influence on the voltage stability. Many numbers of researches are undergoing on dynamic voltage stability of power system to prevent the voltage collapse in the power system which will be lead to blackouts.

In the dynamical analysis, voltage stability can be classified into short term, midterm and long term dynamics based on the time scale of operation. By the name itself, short term dynamics correspond to fast acting devices like generators and induction motors. Midterm and long term dynamics are because of slow acting devices like transformer load tap changers, generator excitation limiters and generator automatic voltage regulators [7].

G. K. Morison, B. Gao, P. Kundar in [16] has showed how voltage instability can occur and the situations in which the modeling of loads, under load tap changers and generator maximum excitation limiters will impact the system voltage stability. Modeling of loads has significant effect on the accuracy of voltage stability analysis [23-24] and investigated the dynamic nature of voltage instability considering dynamic load. To study dynamic voltage stability of a system we need to consider dynamic model for all the elements in the power system [25] and capture all the dynamics of different elements in the system to find out the exact reason for voltage collapse. In [26] voltage instability is associated with tap-changing transformer dynamics by defining the voltage stability region in terms of allowable transformer settings. In [27] they have employed a nonlinear dynamic model of OLTC, impedance loads and decoupled reactive power voltage relations to reconstruct the voltage collapse phenomenon and developed a method to construct stability regions. In [29] analyzed dynamic phenomenon of voltage collapse by dynamic simulations using induction motor models has been analyzed and it explains how voltage collapse starts locally at weakest node and spreads out to the other weak nodes.

Cat S. M. Wong, Parviz Rastgoufard and Douglas Mader in [30] used real time simulation computing facilities to determine and detect signs and patterns of power system dynamic behaviors.

1.4 Historical Review of Major Blackouts

There are several major blackouts that have occurred in last half century. All the reports published on blackouts stated that even though the system is designed for N-1 contingencies, it is still not enough to secure the system operations. The following are some of the major blackout events reported properly.

The first major blackout reported was on November 9th 1965 in United States [31, 32]. Because of heavy loading conditions one out of five transmission lines tripped by backup relay low load level setting. Thus tripping the remaining four transmission lines and diverted 1700MW load from other lines by over loading them and caused voltage collapse. This blackout effected 30 million people and New York City was in darkness for 13 hours. A special issue [33] published in 2005 talks about changes made in power technology and policy after forty years from blackout occurred in 1965.

Blackout on July 13th 1977 occurred in US [31] because of collapse in Con Edison System. A thunder storm lightning strike hit the two transmission lines and a protective equipment malfunction tripped the three out of four transmission lines. This situation increasingly overloaded all the transmission line for 35 minutes and all of them opened. After 6 minutes whole system was out of operation. This blackout left 8 million people in darkness including New York City and took 5 to 25 hours to restore the whole system.

July 23rd 1987 blackout in Tokyo [31]. This blackout occurred because of high peak demand due to extreme hot weather conditions. The increased demand gradually reduced the voltage of 500KV system to 460KV in five minutes. The constant power characteristic loads like Air Conditioning systems gradually reduced the voltage and caused dynamic voltage collapse. Tokyo blackout affected 2.8 million customers with 3.8GW of outage. The whole system was recovered in 90 minutes after the voltage collapse.

Blackout on July 2nd 1996 in United States Western North American power system [31] due to short circuit of a 1300km series compensated 345KV transmission line by flashover to a tree. This blackout affected 2 million people by loss of 11,850MW of load loss.

US Canadian Blackout on August 14th 2003 [31,34]. This started with a 345KV transmission line tripping due to a tree contact. Another line touched a tree after the first line was disconnected. At the same time the computer software designed to warn operators was not functioning properly. All these reversed the power flow and caused a cascading blackout of entire region. During this voltage collapse 400 transmission lines and 531 generating units at 261 power plants tripped. This blackout affected 50 million people by 63GW of load interruption.

The Europe blackout on November 4th 2006 [35] in UCTE (Union for the Coordination of the Transmission of Electricity) inter connected power grid which coordinates 34 transmission system operators in 23 European countries. This blackout started with a 380KV transmission line tripping. This blackout affected 15 million people in Europe and 14.5 GW of load was interrupted in more than 10 countries.

1.5 Scope of this Work:

This research continues the previous research completed at Tulane University by Dr. Sze Mei Wong and Dr. Parviz Rastgoufard on "Unification of Angle and Magnitude Stability to Investigate Voltage Stability of Large-Scale Power System" [38, 30, 36].

The main goal of this thesis is to detect the voltage collapse ahead of time to provide the operators a lead time for remedial actions and for possible prevention of blackouts. To detect cases of voltage collapse, we used pattern recognition and real time simulation case studies and developed heuristic methods for separating voltage stable from voltage unstable cases that result in response to system contingencies and faults. Using Real Time Simulator in Entergy-UNO Power & Energy Research Laboratory, we simulate several contingencies on IEEE 39-Bus Test System and compile the results in two categories of stable and unstable voltage cases. This study

is performed by simulating contingencies at different locations in IEEE 39- Bus Test System for detecting stable and unstable cases. A model is built to examine and identify the stability patterns using artificial neural networks and pattern recognition techniques. This is done by training the artificial neural networks by known stable and unstable training set test cases. Final stage deals with the training of the controllers in order to detect stability of power system in advance by using the trained artificial neural network from the training test cases.

Chapter 2

Background and Mathematical Model

2.1 Voltage stability and Transient stability:

The previous chapter has already given some idea about the voltage stability phenomenon. This chapter discusses about the transient stability, voltage stability and methods to determine these stabilities. Transient stability mainly deals with generator dynamics and voltage angles. But voltage stability deals with loads and voltage magnitudes. This chapter will discuss about the traditional techniques for the transient and voltage stability.

2.2 Voltage Stability:

Voltage is considered as an integral part of power system and is considered as an important aspect in system stability and security. In recent years problem of voltage instability got a considerable attention because of many voltage collapse incidents.

2.2.1 Basic concepts of voltage stability:

Voltage stability is the ability of power system to maintain steady acceptable voltages at all buses in the system under normal operating conditions, after being subjected to a disturbance [1]. Power system is unstable when voltage decreases beyond particular limit because of outage of equipment, increase in load or decrease in controller's actions. Voltage instability and voltage collapse may be used interchangeably. Mainly voltage stability is the subset of power system stability. Voltage instability normally occurs because of monotonically decreasing voltage.

Voltage stability can be classified in to two sub classes

I. Large disturbance voltage stable.

II. Small disturbance voltage stable

2.2.1.1 Large disturbance voltage stable:

It is mainly concerned with system ability to control voltage after large disturbance like system faults, loss of generators or circuit contingencies occur. This voltage stability depends on load characteristics and the interactions of both continuous and discrete controls and protection. The study period for stability analysis can extend from few seconds to tens of minutes because this analysis requires examination of non linear dynamic performance of a system over a period of time such that it can capture the interaction of devices like ULTCs and generators field excitation limiters etc. Criterion for large disturbance voltage stability involves, following a given disturbance and following system controller actions to control voltages at all the buses to acceptable steady state levels.

2.2.1.2 Small Disturbance Voltage Stable:

This will deal with the system ability to control voltages following small disturbances like change in load. This form of stability depends on characteristics of load and discrete controls at a given point of time. Basic process contributing for small disturbance voltage instability is of steady state in nature. Then static analysis methods can be effectively used to determine stability margins, identify factors influencing stability and examines wide range of system conditions.

An example for small signal voltage stability is that, at a given operating condition for every bus in the system voltage magnitude increases as the reactive power at the same bus

increases. System is said to be unstable if the voltage magnitude at a bus decreases as the reactive power injection at the same bus increases. We can also tell that system is voltage stable if V-Q sensitivity is positive for every bus and unstable if V-Q sensitivity is negative for at least one bus.

2.2.2 Methods of Voltage stability Analysis

2.2.2.1 P-V Curve Analysis

P-V curve analysis is used to determine voltage stability of a radial system and also a large meshed network. For this analysis P i.e. power at a particular area is increased in steps and voltage V is observed at some critical load buses and then curves for those particular buses will be plotted to determine the voltage stability of a system by static analysis approach. The main disadvantage of this method is that the power flow solution will diverge at the nose or maximum power capability of the curve and the generation capability have to be rescheduled as the load increases.

To explain the P-V curve analysis let us assume a simple circuit which has a single generator, single transmission line and a load. This circuit consists of two buses. The one line diagram for this circuit is shown in Figure 2.1.

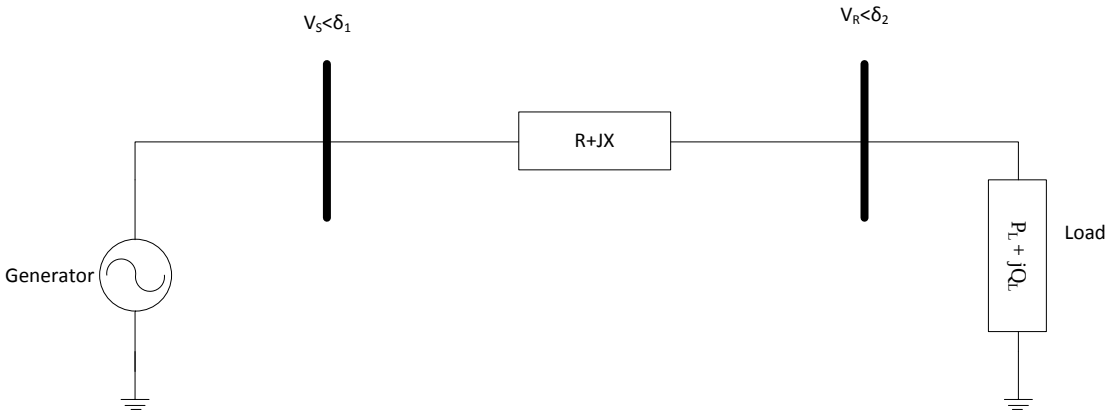

Figure 2.1 A two-bus test system

P-V curves are useful in deriving how much load shedding should be done to establish pre fault network conditions even with the maximum increase of reactive power supply from various automatic switching of capacitors or condensers.

Here the complex load assumed is $S_L = P_L + jQ_L$, where P_L and Q_L real and reactive power loads respectively. V_R is receiving end voltage and V_S is sending end voltage. CosΦ is the load power factor then complex load power can be written as,

$$S_L = |V_R|I^* = |V_R||I|(\cos\Phi + i\ \sin\Phi) = |V_R||I|e^{i\Phi} \qquad (2.1)$$

Let us consider $\beta = \tan\Phi$ then

$$S_L = P_L(1 + i\beta) = Q_L\left(\frac{1}{\beta} + i\right) \qquad (2.2)$$

But from equation (2.1)

$$P_L = |V_R||I|\cos\Phi \qquad (2.3)$$

$$Q_L = |V_R||I|\sin\Phi \qquad (2.4)$$

The network equations for the circuit considered for the case where resistance of transmission line assumed as zero are given below,

$$P_L = \frac{|V_S||V_R|}{X}\sin\delta_{12} \tag{2.5}$$

$$Q_L = -\frac{|V_S|^2}{X} + \frac{|V_S||V_R|}{X}\cos\delta_{12} \tag{2.6}$$

Where $\delta_{12} = \angle\delta_1 - \angle\delta_2$

$$\frac{|V_S||V_R|}{X}\cos\delta_{12} = Q_L + \frac{|V_S|^2}{X} \tag{2.7}$$

From equations (2.6) and (2.7)

$$P_L^2 + \left[\beta P_L + \frac{|V_S|^2}{X}\right]^2 = \frac{|V_S|^2|V_R|^2}{X^2} \tag{2.8}$$

By solving above equation we will get

$$|V_R|^2 = \frac{|V_S|^2}{2} - \beta P_L X \pm \left[\frac{|V_S|^4}{4} - P_L X(P_L X + |V_S|^2\beta)\right]^{\frac{1}{2}} \tag{2.9}$$

The above equations can give P-V curve when the values of V_1 , β, and X are fixed. As we changing P, real power load, we will get two voltage solutions at each loading case. But at P=Pmax the voltage solutions we got are of same value and this voltage is called as critical voltage. If P is increased beyond Pmax then the solution will become unsolvable which will indicate voltage collapse. The P-V curves for $V_1 = 1\angle 0$, X=0.4 p.u and for different power factor are shown in Figure 2.2.

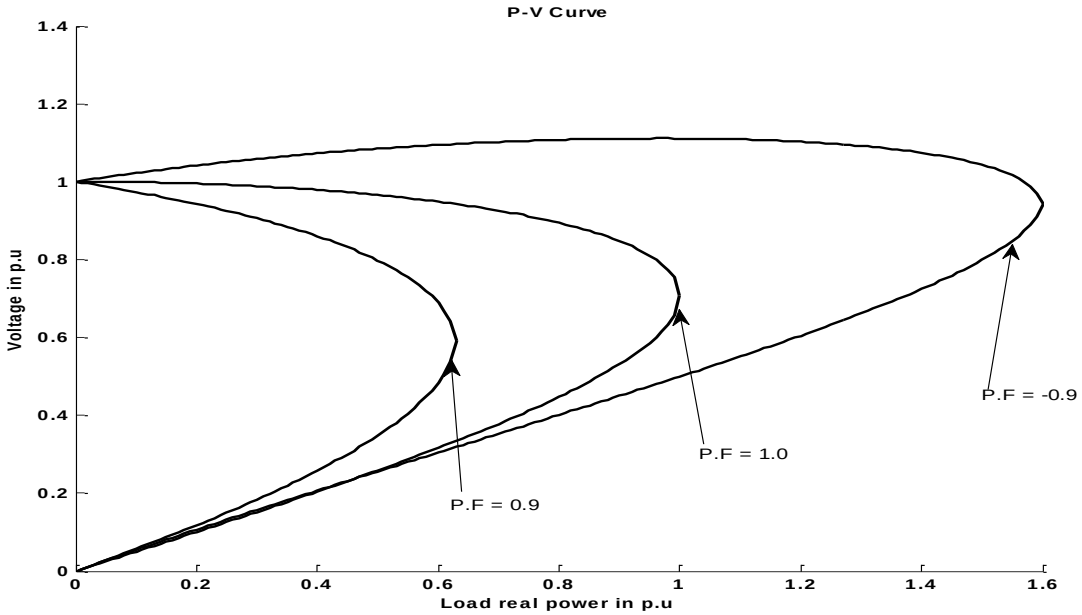

Figure 2.2 P-V Curve

2.2.2.2 V-Q Curve Analysis

V-Q curves plot voltage at a test or critical bus versus reactive power on the same bus. V-Q curves will give good insight in to system reactive power capabilities under both normal and contingency conditions. The V-Q curves have many advantages. V-Q curves will give reactive power margin at a test bus. Reactive power compensation will provide security to voltage stability problems which is determined by plotting reactive power compensations on to V-Q curves. The slope of the V-Q curve will indicate stiffness of the test bus. This method artificially stresses a single bus which should be confirmed by more realistic methods before coming to conclusion.

2.2.2.3 V-Q Sensitivity Analysis

The V-Q sensitivity analysis will give information regarding the sensitivity of a bus voltage with respect to the reactive power consumption. This analysis can provide system wide voltage stability related information and can also identify areas that have potential problems. The linearized steady state power systems equations can be expressed as

$$\begin{bmatrix}\Delta P\\ \Delta Q\end{bmatrix} = \begin{bmatrix}J_{P\theta} & J_{PV}\\ J_{Q\theta} & J_{QV}\end{bmatrix}\begin{bmatrix}\Delta\theta\\ \Delta V\end{bmatrix} \qquad (2.10)$$

Where ΔP= incremental change in bus real power

ΔQ= incremental change in bus reactive power injection

ΔV= incremental change in bus voltage magnitude

Δθ= incremental change in bus voltage angle.

Here the elements of matrix J (Jacobian matrix) will give the sensitivity between power flow and voltage changes.

The general structure of the system model for voltage stability analysis is similar to that of transient stability analysis. The overall system equations, comprising a set of first-order differential equations may be expressed as,

$$\dot{X} = f(X, V) \qquad (2.11)$$

Where X is state vector

V is bus voltage

Rewriting the linear relationship between power and voltage for each device when $\dot{X}$=0 can be expressed as

$$\begin{bmatrix}\Delta P_d \\ \Delta Q_d\end{bmatrix} = \begin{bmatrix}A_{11} & A_{12} \\ A_{21} & A_{22}\end{bmatrix}\begin{bmatrix}\Delta V_d \\ \Delta \theta_d\end{bmatrix} \quad (2.12)$$

Here "d" stands for device.

All the above elements are for a particular device. A_{11}, A_{12}, A_{21} and A_{22} represent system Jacobian elements.

V-Q sensitivity analysis is done by keeping real power P constant and evaluating voltage stability by considering the incremental relationship between Q and V. when ΔP=0 then

$$\Delta Q = J_R \Delta V \quad (2.13)$$

Where

$$J_R = \left[J_{QV} - J_{Q\theta} J_{P\theta}^{-1} J_{PV}\right] \quad (2.14)$$

J_R is called as reduced Jacobian matrix of the system Equation 2.13 can also be written as

$$\Delta V = J_R^{-1} \Delta Q \quad (2.15)$$

Where J_R^{-1} is the inverse of the reduced V-Q Jacobian and its i^{th} diagonal element will provide V-Q sensitivity at bus i.

As mentioned earlier V-Q sensitivity at a bus is the slope of Q-V curve at given operating conditions. A positive V-Q sensitivity is for stable condition and negative is for unstable condition. As stability decreases magnitude of V-Q sensitivity increases and vice versa. Because

of the nonlinear nature of V-Q relationship, the magnitudes of the sensitivities for different system conditions do not provide a direct measure of the relative degree of stability.

2.2.2.4 Q-V Modal Analysis

Eigen values and Eigen vectors of reduced Jacobian matrix J_R will be useful in describing voltage stability characteristics.

Let us consider $J_R = R \wedge L$ (2.16)

Where R= right Eigen vector matrix of J_R

L= left Eigen vector matrix of J_R

Λ=Diagonal Eigen value matrix of J_R

Using modal transformation Equation 2.16 can be written as

$$J_R^{-1} = R\Lambda^{-1}L \tag{2.17}$$

From Equation (2.13)

$$\Delta V = R\Lambda^{-1}L\,\Delta Q \tag{2.18}$$

$$\Delta V = \sum_i \frac{r_i l_i}{\lambda_i}\,\Delta Q \tag{2.19}$$

Here r_i is the i^{th} column right Eigen vector and l_i is the i^{th} row left Eigen vector. Eigen value λ_i and corresponding r_i and l_i define i^{th} mode of Q-V response. Note that

$$R^{-1} = L \tag{2.20}$$

Using Equation 2.19 we obtain

$$L\,\Delta V = \Lambda^{-1} L \Delta Q \qquad (2.21)$$

$$v = \Lambda^{-1} q \qquad (2.22)$$

Where $v = L\Delta V$ is vector of modal volatge analysis and $q = L\Delta Q$ is vector of modal reactive power variations.

From equation (2.22)

$$v_i = \frac{1}{\lambda_i} q_i \qquad (2.23)$$

And Λ^{-1} is diagonal matrix. Details of development of Equation 2.13 to 2.22 in [1].

From above equations it is clear that if $\lambda_i > 0$ then voltage and reactive power of i^{th} mode are along same direction which implies that voltage stable. If $\lambda_i < 0$ voltage and reactive power of i^{th} mode are along opposite direction which implies voltage unstable. Magnitude of λ_i determines degree of stability of i^{th} modal voltage. The smaller the magnitude of positive λ_i means i^{th} mode is closer to voltage instability and vice versa. If $\lambda_i=0$ it means that i^{th} modal voltage collapses.

2.2.2.5 Dynamic Analysis

Dynamic analysis of voltage stability will be same as transient stability because structure for dynamic analysis is going to be the same as transient stability structure. The whole system representation can be done with a set of first order algebraic equations and those equations are

$$\dot{X} = f(X, V) \text{ and}$$

$$I(X, V) = Y_N V \qquad (2.24)$$

With initial conditions (X_0, V_0)

X= State vector of the system

V=Bus voltage vector

I= Current injection vector

Y_N= Network node admittance matrix

By including the action of transformer tap changers and phase shift angle control devices, elements of Y_N change with bus voltage and time. Because of the time dependent nature of Y_N, current injection vector I also becomes time dependent in all equations representing the whole system. These equations can be solved in time-domain by any of the numerical integration techniques and network power flow analysis methods. These techniques take several minutes depending upon the computer speed. By including slower system dynamics which lead to voltage collapse will increase the stiffness of differential equations representing system as we compared to transient stability model. These kinds of differential equations can be solved by implicit integration methods.

2.3 Rotor Angle Stability

According to P. Kundur [1] rotor angle stability is the ability of connected synchronous machine power system to remain in synchronism. This stability mainly concentrates on rotor angle oscillations of the synchronous machine as the power output changes.

The relation between power transferred and rotor angle of a synchronous machine which is non linear in nature can be derived from the below given single machine infinite bus system

(SMIB). This circuit represented by Figure 2.3 has two buses connected by two transmission lines of reactance X_1 and X_2.

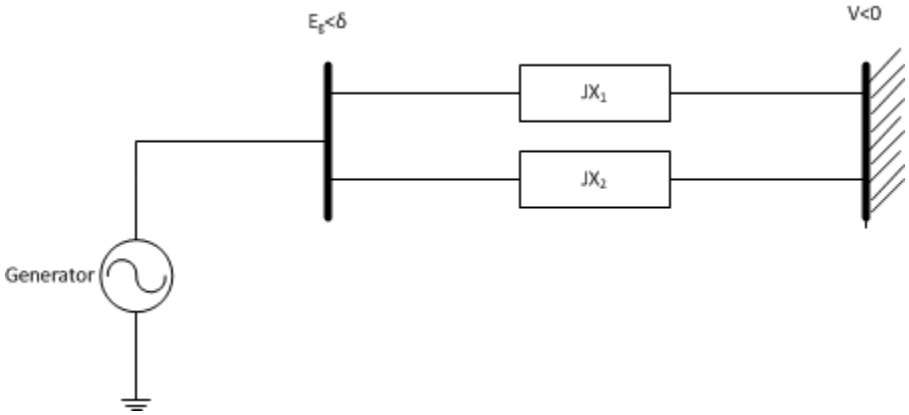

Figure 2.3 Single machine infinite bus system

Here the power transferred from generator to infinite bus is a function of angular separation between the rotor of a machine and the infinite bus voltage angle. Neglecting transmission line losses, the relationship between real power and swing angle is

$$P = \frac{E_g V}{X_T} \sin \delta \qquad (2.25)$$

Where $X_T = X_G + X_1 || X_2$

By considering suitable values for E_g, V and X_T power versus angle plot is shown below.

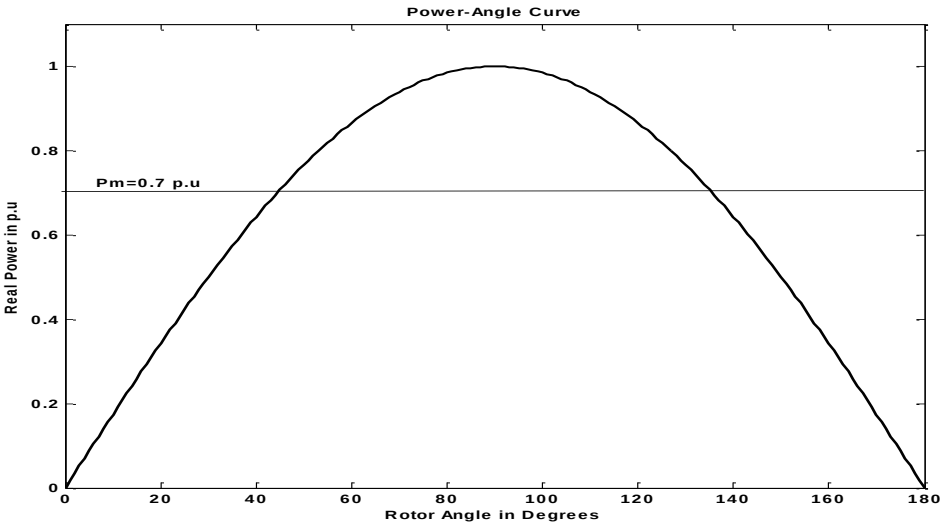

Figure 2.4 Power-Angle curve

By considering in plot of Figure 2.4, it is seen that, power transferred will be zero when rotor angle is zero, it increases to maximum as the δ increases up to 90^0 and a further increase in δ results in decrease in power transfer. For more than one machine systems their relative angle displacement affects the interchange of power in a similar manner.

The rotor angle stability of a system can be divided in two categories of small signal stability and transient stability.

2.3.1 Small Signal Stability

This is also called as small disturbance stability which is the ability of power system to maintain synchronism under small disturbances. These disturbances are originated from small variations in loads and generation. The instability which may be resulted from these variations will lead to two forms, one is steady increase in rotor angle due to lack of synchronizing torque and second one is rotor oscillations of increasing amplitude due to lack of sufficient damping

torque. Small signal stability depends on initial operating conditions, Strength of transmission system and type of generation excitation controls.

2.3.2 Transient Stability

Transient stability is the ability of power system to maintain synchronism when subjected to severe transient disturbances [1]. This stability depends on both the initial conditions and initial operating state of the system and the severity of the disturbance. For the severe faults in transient stability the system state is altered so that the post disturbance steady state operation differs from the pre fault state. In interconnected large power systems transient instability may not occur in first swing because it may be the result of the superposition of several methods of oscillations. Transient stability studies will be done for 3 to 5 seconds following a disturbance. Sometimes it may be extended to 10 seconds for large systems.

By using the small system which is SMIB considered earlier to describe the transient stability. For simplicity generator is represented by the classical model and the speed governor effects are neglected. Generator voltage behind the transient reactance $X_d^{|}$ is denoted by $E^{|}$. Rotor angle δ represents the leading angle between $E^{|}$ and E_B. When a disturbance occurs on the system then $E^{|}$ remains constant but δ changes as the rotor speed deviates from synchronous speed w_0. The generation equation of motion which is also called as swing equation will be

$$\frac{2H}{\omega_0}\frac{d^2\delta}{dt^2} = P_m - P_{max}\sin\delta \qquad (2.26)$$

P_m = mechanical power

H = inertial constant MW.S/MVA

δ = rotor angle in electric radians

t= time in seconds

2.3.3 Methods of Transient stability analysis

2.3.3.1 Equal Area Criterion

Equal area criterion can determine the transient stability of a system without solving for swing equation. This technique will calculate the information needed for transient stability arrangement from the power angle curve. Equal area criterion requires following relations [1].

$$P_e = \frac{EV_\infty}{X} \sin \delta \tag{2.27}$$

$$\dot{\delta} = \omega \tag{2.28}$$

$$\dot{\omega} = \ddot{\delta} = \frac{1}{M}(P_m - P_e) \tag{2.29}$$

P-δ curve for the system described earlier is shown Figure 2.5.

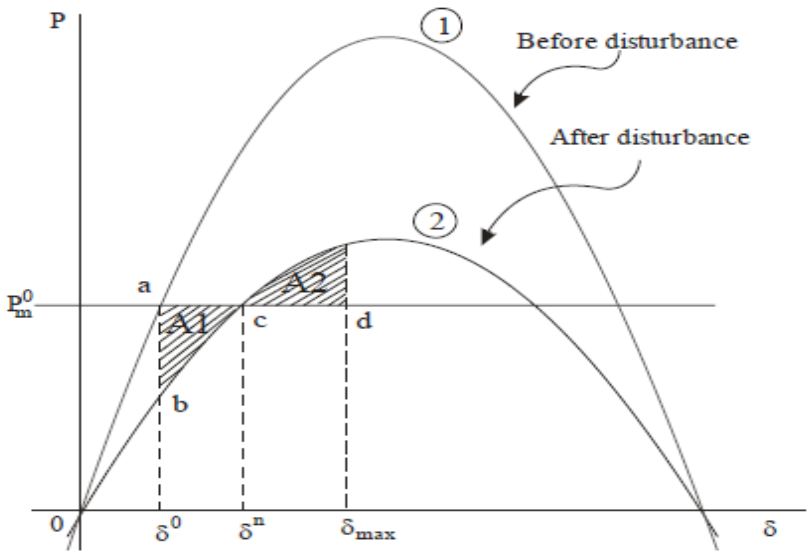

Figure 2.5 Equal area criteria

Curve (1) represents a pre disturbance situation and P_m^0 is the mechanical input power to the generator in steady state and equal to P_e in steady state. It is assumed that constant mechanical input power, damping is neglected, and classical machine model.

According to the assumption of constant mechanical input power to the generator will be P_m^0through out the transient and post disturbance. Point 'a' in figure 2.5 represents the steady state operating point and $\dot{\delta}$ is the steady state rotor angle of the system.

If a fault occurs on one of the transmission line and assume that the line has been disconnected by protective elements in the system then, for one of the line outage impedance of power flow path increases and the maximum power transfer capability decreases which can be realized from the below equation.

$$P_{max} = \frac{EV_\infty}{X_T} \qquad (2.30)$$

Curve 2 in the figure 2.5 reflects the one line outage case for the considered system. Point 'b' is the operating point for the one line outage case. But the rotor angle cannot change instantaneously because of moment of inertia of the rotor. Now for line outage case P_m is greater than P_e which is point 'b' on curve 2. Rotor will accelerate until the operating point reaches point 'c' on curve 2. At this operating point rotor angle is δ^n and $P_m = P_e$. But here the rotor speed higher than synchronous speed, hence rotor angle continues to increase. But for rotor angle greater than δ^n, electric power P_e is greater than P_m and the rotor tries to decelerate. At point 'd' on curve 2 rotor attains its synchronous speed ω_0. But still P_e is greater than P_m so that rotor continues to decelerate and reaches point 'b'. The rotor will oscillate indefinitely about the new equilibrium point δ^n because there is no damping in the system.

The kinetic energy stored in the system when the rotor is accelerating can be shown by the shaded area A_1 and this is

$$A_1 = \int_{\delta^n}^{\delta^0} (P_m - P_e)\, d\delta \qquad (2.31)$$

The decelerating energy of the system is shown in shaded area A_2 and that is

$$A_2 = \int_{\delta^n}^{\delta^{max}} (P_m - P_e)\, d\delta \qquad (2.32)$$

Transient stability will be determined from areas A_1 and A_2 .

I. When $A_1 > A_2$ system is unstable

II. If $A_1 < A_2$ system is stable

III. For $A_1 = A_2$ critical angle and critical clearing time can be determined for the system.

2.3.3.2 Numerical Integration Techniques

From the last discussion it can be stated that total power system can be represented as

$$\dot{X} = f(X, V, t) \qquad (2.33)$$

Here X is the state vector of n dependent variables and t is independent variable. The main goal of the numerical integration techniques is to solve for X as a function of t with the given initial conditions. Depending upon the method using some approximation will be applied to the solution method. The main methods used in numerical techniques are Euler's method and Ranga-Kutta method.

2.3.3.3 Transient Energy Function Approach

TEF is one of the direct methods to determine the transient stability of a system without solving for different equations. This method uses transient energy to determine the transient stability of the power system. The approach in TEF method for power system is equivalent to a ball rolling on the inner surface of a bowl [39, 40]. Initially consider the power system is operating at stable equilibrium point and it is equivalent to ball resting at the bottom of the bowl. When a fault occurs on the power system then system will accelerate and gains some kinetic energy and it moves away from SEP and it is equivalent to ball moving away from its resting point when some external force is applied on it. After the fault is cleared the kinetic energy gained during fault on period will be converted in to potential energy same as the ball rolling up the potential energy surface. The system has to absorb the kinetic energy to avoid instability because this kinetic energy will try to bring the generators towards a new equilibrium point which is unstable. This potential energy absorbing capabilities depends on post disturbance system. Transient energy function method can be explained well with the figure (2.6).

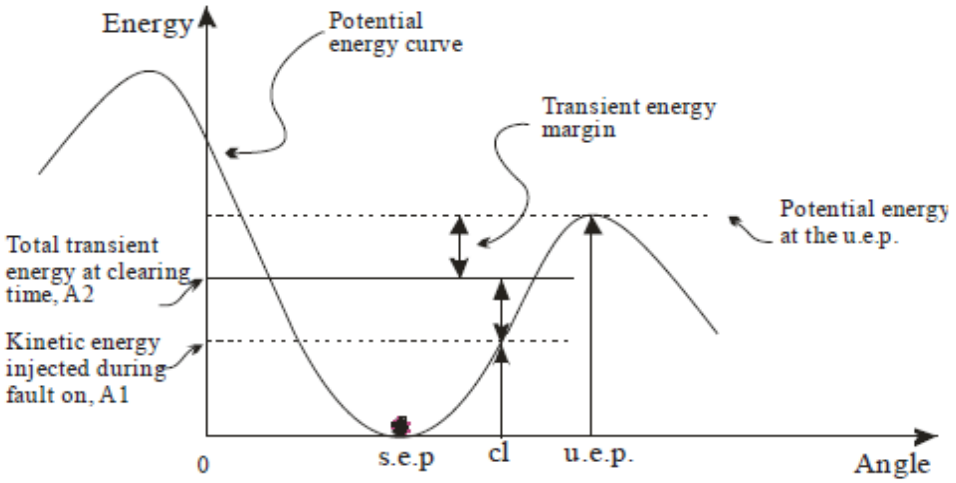

Figure 2.6 Transient energy function approach

The curve represents potential energy of the system. Area A_1 is the kinetic energy gained when the system is having a fault and δ_c is the fault clearing rotor angle. Area A_2 is the total energy present in the system at clearing angle δ_{cl}. If the post fault system can convert the excessive kinetic energy then the system is said to be stable that is kinetic energy at clearing time plus the potential energy clearing time is less than the potential energy of a unstable equilibrium point. This can be shown in equation form as

$$V_{KE}(\delta_{cl}) + V_{PE}(\delta_{cl}) < V_{PE}(\delta_{uep}) \qquad (2.34)$$

If the above condition does not satisfy then the system is unstable.

2.4 Unification of Voltage and Angle Stability

As mentioned in chapter 1, this research is continuation of research done by Dr. Sze Mei Wong and Dr. Parviz Rastgoufard at Tulane University on "Unification of Angle and Magnitude Stability to Investigate Voltage Stability of Large-Scale Power System". This part of the chapter will give some detailed idea on unification approach and how it is used to predict voltage stability from angle stability of a power system.

Dynamic systems with multiple time scales arise naturally in many domains. Here we are interested in system of Differential equations in R^{m+n} of the form

$$\dot{x} = f(x, y, P) \qquad (2.35)$$

$$\dot{y} = \varepsilon g(x, y, P) \qquad (2.36)$$

These systems are called singularly perturbed differential equations or fast slow vector fields [26]. Here $\varepsilon \geq 0$ is a small parameter, x variables are called as fast variables, y variables are called as slow variables, and these two systems have time variables t and T with dT/dt=ε.

A power system is highly nonlinear system and is dynamic. Power system stability problems can be modeled as a fast-slow nonlinear system due to interaction of mechanical and electrical time constant. If a power system is represented by Equation (2.34), Equation (2.35) then x stands for the state variables of the system and those are rotor angles and rotor speed, y represents algebraic variables which are slow and those are bus voltage magnitudes and voltage angles. P is the parametric variables like real and reactive power injections at each bus [38].

If $\varepsilon \rightarrow 0$ the $\dot{y} = 0$ which means y becomes a constant value,

$$\dot{x} = f(x, c, p) \tag{2.37}$$

Equation 2.37 resembles the differential equation used for transient stability studies while changes of the algebraic variables y are neglected. Solving function f gives equilibrium points of transient response of the system under different loading conditions. The transient solutions are X_t^{p1}, X_t^{p2},…., X_t^{pmax} and any value larger than P_{max} result in transient unstable. Here "t" stands for transient solution. By linearizing the differential equation it will become as $\dot{x} = Ax$ where A is system matrix. If all the eigenvalues of the A matrix have negative real parts, the system is considered as transient stable.

When $\frac{1}{\varepsilon} \rightarrow 0$, g(x,y,p)=0 and x becomes as constant value.

$$g(c, y, p) = 0 \tag{2.38}$$

Above equation represents the steady state response of a power system. By solving the above equation we will get steady state value of the variable vector and the solution under different loading conditions can be expressed as X_v^{p1}, X_v^{p2},…., X_v^{pmax}. Linearizing the function g algebraic equation will become as,

$$\begin{bmatrix} \dot{\Delta x} \\ 0 \end{bmatrix} = J \begin{bmatrix} \Delta x \\ \Delta y \end{bmatrix} \tag{2.39}$$

Where J is the unreduced Jacobian matrix, $J = \begin{bmatrix} f_x & f_y \\ g_x & g_y \end{bmatrix}$

If all the Eigen values of J are negative then the system is considered as voltage stable.

There is a correlation between the solutions from transient stability and that of voltage stability [38]. Form eq (2.36) which represents transient stability, by setting $\dot{x} = 0$ indicates dynamcis have vanished and system reached its equilibrium state. This can be represented by set of non linear algebraic equations

$$f(x_{eq}, y_{ss}, p_{ss}) = 0 \tag{2.40}$$

And for a specific equilibrium point

$$g(x_a, y_a, p_a) = 0 \tag{2.41}$$

x_{eq}, y_{ss} and p_{ss} are variables from transient stability and they can be obtained in less than a minute, while x_a, y_a and p_a are variables from voltage stability and it usually takes 30 minutes to obtain them. If X_{eq} can predict x_a, y_{ss} can predict y_a and p_{ss} can predict p_a then 30 minutes result can obtained in one minute.

2.5 Pattern Recognition

According to Duda and Hart [41], "pattern recognition is act of taking in raw data and taking an action based on the category of the pattern". A pattern is a type of reoccurring event or object which can be named. Finger print image, hand written word, speech, etc can be considered as a pattern. The process of recognition is a machine classification and assigns the given objects to prescribed classes. Figure (2.7) illustrates the flow chart pattern recognition model development and data classification.

Pattern recognition techniques are used in engineering applications like wave form classification where wave forms corresponding to one class of data are discriminated from the data corresponding to a different class. We are using pattern recognition techniques to distinguish voltage stable waveforms from voltage unstable waveforms. Regularized least-squares (RLS) classification is used for our binary classification problem. RLS is a learning method that obtains solutions for binary classification problems.

By looking at Figure 2.7 it can be observed that pre processing will be take place on the training set and test set acquired data and is forwarded to feature extraction purpose. Features will be choosed on the given data. These choosed features from the training set data is used to build an optimized model for estimation. Later this model will be used to classify the patterns of the test set data.

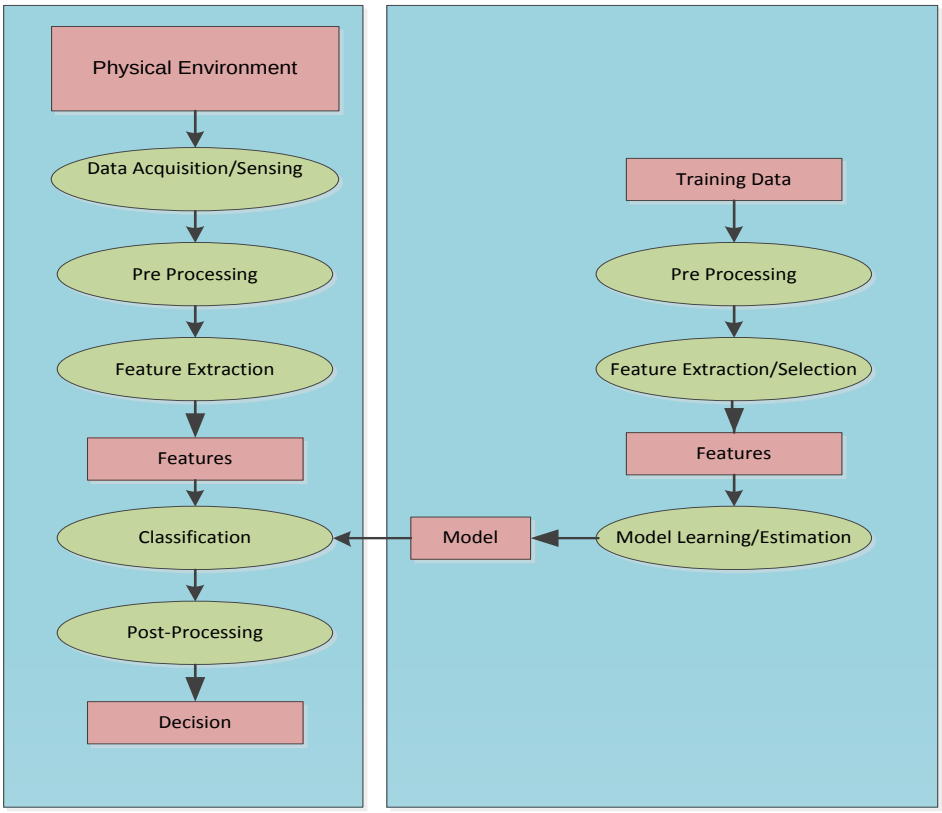

Figure 2.7 Flow Chart of Pattern Recognition Model [38]

2.5.1 Regularized Least-Square Classification (RLSC)

As mentioned earlier RLSC is a learning method that obtains solution for binary classification via Tikhonov regularization in a Reproducing Kernel Hilbert Space using the square loss function [42-43]. Let's assume X and Y are two sets of random variables and training set for pattern classification is S = (x_1, y_1), …., (x_n, y_n) and it satisfies $x_i \epsilon R^n$ and $y_i \epsilon \{-1, 1\}$ for all i. the main goal is to learn a function *f(x)* while minimizing the probability of error described by Equation 2.42.

$$\Pr\left(sgn\left(f(x)\right)\right) \neq y \qquad (2.42)$$

To minimize the error we can use Empirical Risk Minimization (ERM) and obtain M_1 such that

$$M_1 = \min_{f \epsilon H} \frac{1}{n} \sum_1^n \big(y_i - f(x_i)\big) \qquad (2.43)$$

Above problem is ill defined, because the set of functions required in minimizing Equation 2.43 are not considered. By representing function f lie in a bounded convex subset of a Reproducing Kernal Hibert Space H that simultaneously has small empirical error and small norm in reproducing Kernel Space generated by kernel function K. The resulting minimization problem can be solved via Lagrange multipliers.

$$\mathrm{M}_2 = \min_{f \epsilon H} \frac{1}{n} \sum_1^n \big(y_i - f(x_i)\big)^2 + \lambda \|f\|^2{}_k \qquad (2.44)$$

Whereas $\|f\|^2{}_k$ is the norm in the hypothesis space defined by kernel k.

The solution for Tikhonov regularization problem can be solved by Representer Theorem [48, 49] and it is:

$$f(x) = \sum_{i=1}^n c_i k(x, x_i) \qquad (2.45)$$

Learning algorithm for this problem is very simple. First kernel matrix K is constructed from training set S.

$$K = \big(k_{ij}\big)_{1 \le i,j \le n} \qquad k_{ij} = k\big(x_i, x_j\big)$$

Next step is to compute the vector coefficients c= $(c_1, c_2, \ldots, c_n)^T$ by solving the system of linear equations

$$(K + n\lambda I)c = y \qquad (2.46)$$

$$c = (K + n\lambda I)^{-1} y \qquad (2.47)$$

Where y= $(y_1, \ldots, y_n)^T$ and I is the identity matrix of dimension n and finally classifier is,

$$f(x) = \sum_{i=1}^{n} c_i k(x, x_i) \qquad (2.48)$$

The sgn (f(x)) will give the predicted label (-1 or +1) for the instance x and magnitude of f(x) is the confidence in this prediction.

Chapter 3

HYPERSIM and EMTP-RV

This chapter will explain about HYPERSIM and EMTP-RV environment and in build models and hardware structure of Hypersim and EMTP-RV.

3.1 Introduction to HYPERSIM real time simulator

HYPERSIM is fully digitalized real time power system simulator. It can simulate various kinds of power system networks to study about the dynamic stability and electromagnetic transients. Hypersim has large number of in-built models (Libraries), like synchronous machines, motors, different types of loads, control equipment like breakers, HVDC and SVC. Its hardware is designed by SGI and the software is by Hydro-Quebac Research Institute (IREQ).

Hypersim will also allow building or developing custom models and control equipment for the power system networks. It will offer great flexibility with different types of simulators and software's like MATLAB/SIMULINK, EMTP software in such a way that importing or exporting the models between Hypersim and others is possible. The main advantage of Hypersim is its real time simulation with the help of parallel processing technology. Real time simulator is a simulator that can synchronize simulation time in the computer with the time in the real world. This means one second in simulator is equal to real worlds one second. For real time simulations Hypersim uses parallel feature of any power transmission to effectively divide the power system network into parallel tasks and will distribute the tasks between parallel processors. Hypersim can also communicate with I/O devices to control the actual real components of power systems for closed loop testing.

3.1.1 HYPERSIM Hardware Environment

Hypersim's hardware environment requires two types of different platforms to execute power system networks. One is HYPERSIM WORKSTATION and the other one is HYPERSIM REAL TIME COMPUTATION ENGINE.

Hypersim workstation is a computer which can interact with the simulator. It can be one of two types from the below mentioned workstation types.

i. Standard PC based on Linux Redhat 7.2/7.3

ii. Sun workstation based on UNIX Solaris 5.6/5.8

Hypersim Real time computation engine is a parallel processing simulator and is one of the two types and each of them has their own advantages and disadvantages.

i. SGI super computer (family of 2000, 3000, 300).

ii. PC cluster (A group of standard Intel processors).

3.1.2 HYPERSIM Software Environment

Hypersim software consists of many tools for the real time simulation and real equipment tests and they are

HYPERSIM: It is a graphical interface to edit and control the power systems to simulate.

HYPERVIEW: This is a GUI tool for Netlist, Load flow and Snapshot.

SCOPEVIEW: It is the acquisition tool which can show the results as graphs.

MATLAB/SIMULINK: It is famous for control systems design and simulation.

HYMONITOR: This will monitor the performance of parallel processors.

TESTVIEW: Testview is for automatic control and testing of the simulator.

SI5: This one is a database to store all types of results.

3.2 EMTP-RV

EMTP-RV is the end result of the "EMTP Restructuring project" taken by the DCG (Development Coordination Group) in 1998 for modernizing the EMTP96 software. EMTP-RV is the enhanced computational engine and EMTPWorks is its new graphical user interface. It is well proven, comprehensive and sophisticated program for the simulation of electromagnetic, electromechanical and control systems transients in multiphase electric power systems. It features a wide variety of modeling capabilities encompassing electromagnetic and electromechanical oscillations ranging in duration from microseconds to seconds. The data transmission from EMTPWorks to EMTP-RV is done by Netlist file. This Netlist file is used by EMTP-RV to decode the simulated network topology, finds all required device models and computation functions, builds the system matrix and performs the simulation. Results will be stored into binary and ASCII files. A software named as Scopeview is used to view the binary output files as waveforms. EMTP uses nodal analysis and solves the system differential equations using fixed time-step trapezoidal with/without backward Euler method. The outcome of EMTP simulation is very efficient and that's why EMTP is one of the best tools for solving large network.

3.3 Power system components in HYPERSIM and EMTP

As mentioned this chapter is going to discuss about the Hypersim and EMTP in building power system models. The models we are going to discuss will represent the generalized models for Hypersim and EMTP. We are going to discuss about synchronous generators, excitation system, stabilizer, transmission lines, transformers, loads especially dynamic loads. This discussion will be started with generator section.

3.3.1 Synchronous Generator

The synchronous generator model in Hypersim is implemented by the Park's (DQ) equations using sletz's method [44]. There are two equations and one is D-axis equation and other one is Q-axis equation. The block diagrams for D and Q axis are shown below and the parameters in the block diagram are explained after the diagram. These parameters will be the same for EMTP.

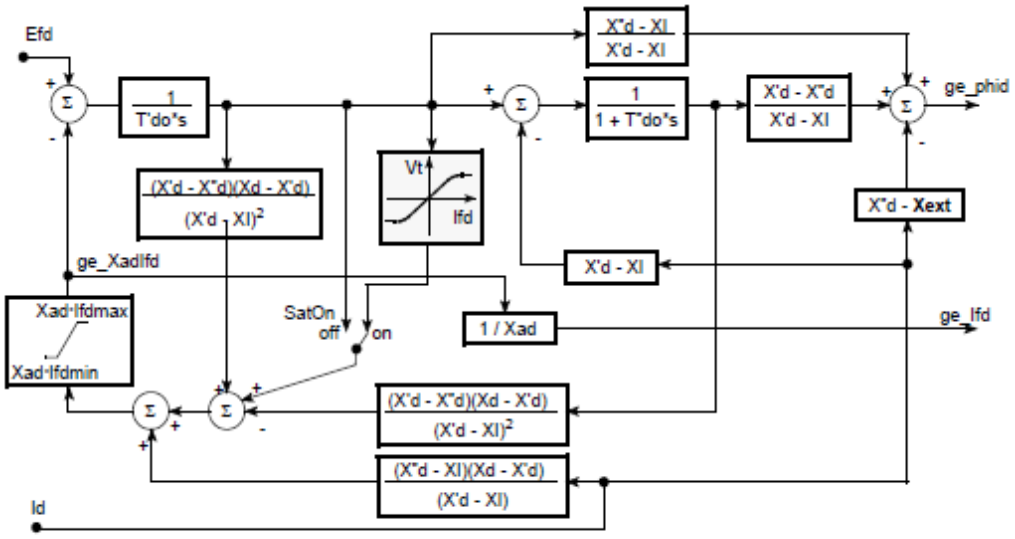

Figure 3.1 Generator D-axis Block diagram [44]

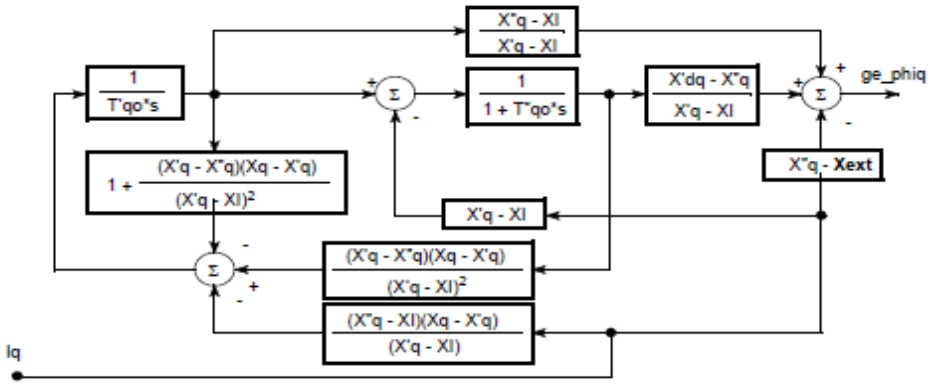

Figure 3.2 Generator Q-axis Block diagram [44]

X_1-Armature leakage Reactance

R_a-Armature resistance

X_d-Direct synchronous reactance

$X_d^{'}$-Direct transient reactance

$X_d^{''}$-Direct sub-transient reactance

X_q-Quadrature synchronous reactance

$X_q^{'}$-Quadrature transient Reactance

$X_q^{''}$-Quadrature sub-transient reactance

$T_{d0}^{'}$-Direct axis transient time constant

$T_{d0}^{''}$- Direct axis sub-transient time constant

$T_{q0}^{'}$- Quadrature axis transient time constant

$T_{q0}^{''}$- Quadrature axis sub-transient time constant

Synchronous generator system will ask for some more parameters like base values for the machine, voltage reference, active and reactive power reference. Voltage reference section of the synchronous generator consists of two different selections. One is directly giving the voltage reference value in to the control panel and other selection is reference voltage is equal to required terminal voltage of the generator. That is reference signal for the excitation system is calculated

to have required terminal voltage at the generator terminals. To calculate these values it requires Active and reactive power references.

Synchronous generator control panel has one more section for load flow values. It will ask for type of bus that is slack or generator bus, voltage magnitude, voltage angel, active power and reactive power limits. If the generator is connected to a slack bus then the active power delivered by the generator is calculated by load flow solution and voltage angle is zero (reference bus).

3.3.2 Excitation System

Excitation system controls the terminal voltage of a synchronous machine. This will allow regulating the voltage at terminals of machine or on the high side of step up transformer. This regulation is done by varying the field voltage of the synchronous machine. That is based on the difference between the desired reference voltage and the actual voltage at the terminal at that particular instant. Excitation system consists of two sections one is excitation and other one is regulating system. Excitation system block diagram is given below and the parameters in the block diagram are explained after that.

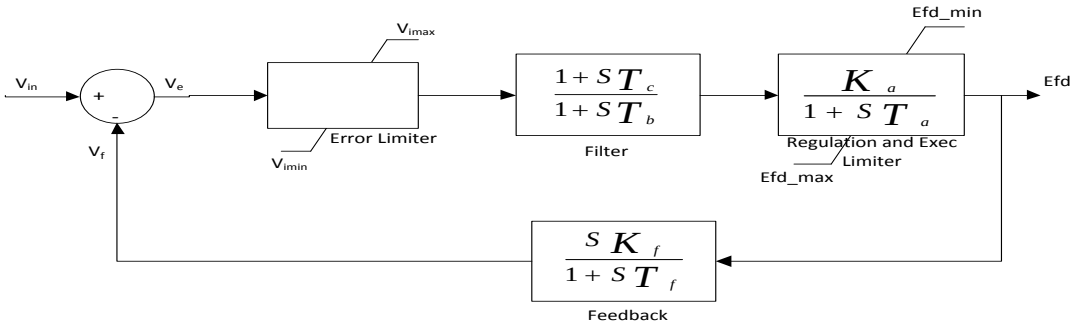

Figure 3.3 Excitation system block diagram

V_{in}-Control input

V_e-Control error

V_f-Feedback voltage

E_{fd}-Field voltage

T_a-Time constant of regulator

T_b-Time constant (lead) of transient filter

T_c-Time constant (lag) of transient filter

K_a-Gain of regulator

K_f-Gain of feedback

Vimin, Vimax-Loop error limits

Efd_min, Efd_max-Execitation voltage limits

From the block diagram it can be observed that excitation voltage to the exciter field of the generator is limited between Efd_min and Efd_max.

3.3.3 Stabilizer

This system is mainly designed to damp the electromagnetic oscillations. The output of the stabilizer is given to excitation system so that it can control the field voltage at the time of transients. Inputs for stabilizer are P_e or Pe_f (filtered electric power) and gate opening signal. Here P_e is for steam turbine and is the electric power with no filtering and Pef is for hydraulic machine and is the electric power with filtering. Block diagram for the stabilizer is given below and the parameters are explained later.

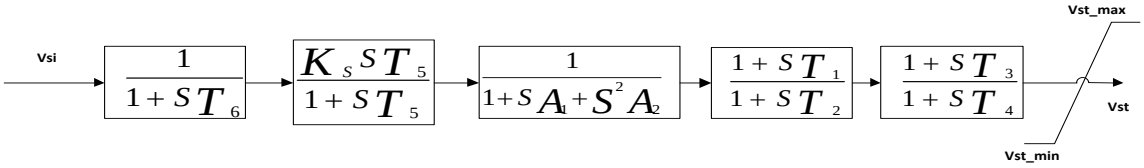

Figure 3.4 Power system stabilizer (PSSA1) IEEE std 421.5 1992, Chap. 8

3.3.4 Transmission lines:

Hypersim and EMTP consist of different types of transmission lines like frequency constant distributed parameter lines and Pi lines. Pi lines are mainly used for short length transmission lines. Both types of transmission lines have coupled lines. All of these different types of transmission lines ask for same common parameters like length of transmission line, RLC parameters distribution type that is transposed or un-transposed, transformation matrix and RLC values for different sequences i.e positive, negative and zero sequence.

If the line is a transposed line then Hypersim and EMTP will take its own inbuilt transformation matrix but if the line is an un-transposed line then user has to give transformation matrix T_i values. If the line is a transposed line then negative sequence parameters values will cancel out and it won't ask for those parameters. These softwares will ask in such a way that 0, 1, 1 modes which means zero, positive, positive. If it is a un-transposed line then modes for RLC is named as 1, 2, 3 which is mean by zero, positive, negative. All the zero, positive and negative sequence values required have to mentioned in per unit if user selects per unit system in the control panel of transmission line. Hypersim can also accept EMTP(.PUN) file as input instead of transformation matrix and RLC parameter values.

This thesis test system is using single frequency constant distributed parameter lines and Pi lines. All the transmission lines are assumed as transposed lines.

3.3.5 Loads

Hypersim and EMTP has different types of load models. They are dynamic load, harmonic load, arc furnace, DC motor and induction motor. Harmonic load is specially used to include harmonics in the power system to represent actual conditions in real world. Dynamic

load is a particular type of load in which active and reactive powers varies as a function voltage and frequency at a point where the load is connected. This load model correctly reproduces the behavior of slow modulations in voltage by the power system dynamics and fast transients introduced by switching phenomenon.

Chapter 4

Test System

4.1 IEEE 39 Bus Test system:

The IEEE 39 BUS (NEW ENGLAND) equivalent power system is used to study the voltage stability dynamics. This test system has a total of 39 buses of which 10 buses are generator buses and this system has a total of 19 loads at different buses. IEEE 39 BUS system also consists of 12 transformers, 10 generators and 34 transmission lines. This system is shown in figure (4.1). This chapter will give the information about the test system in a form that HYPERSIM and EMTP can accept the data.

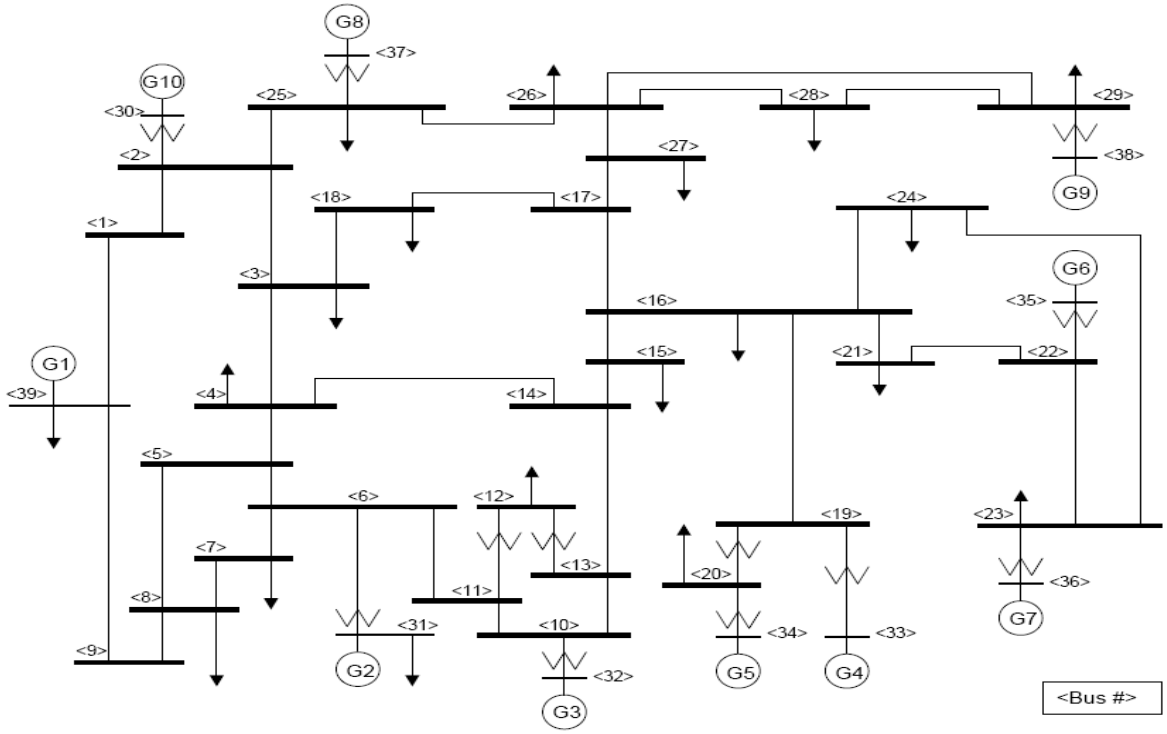

Figure 4.1 IEEE 39Bus system [45]

4.2 Transmission Lines

Table 4.1 Transmission line data

LINE	Resistance PU	Reactance PU	Suceptance PU
1 to 2	0.0035	0.0411	0.6987
1 to 39	0.001	0.025	0.75
2 to 3	0.0013	0.0151	0.2572
2 to 25	0.007	0.0086	0.146
3 to 4	0.0013	0.0213	0.2214
3 to 18	0.0011	0.0133	0.2138
4 to 5	0.0008	0.0128	0.1342
4 to14	0.0008	0.0129	0.1382
5 to 6	0.0002	0.0026	0.0434
5 to8	0.0008	0.0112	0.1476
6 to 7	0.0006	0.0092	0.113
6 to 11	0.0007	0.0082	0.1389
7 to 8	0.0004	0.0046	0.078
8 to 9	0.0023	0.0363	0.3804
9 to 39	0.001	0.025	1.2
10 to 11	0.0004	0.0043	0.0729
10 to 13	0.0004	0.0043	0.0729
13 to 14	0.0009	0.0101	0.1723
14 to 15	0.0018	0.0217	0.366
15 to 16	0.0009	0.0094	0.171
16 to 17	0.0007	0.0089	0.1342
16 to19	0.0016	0.0195	0.304
16 to 21	0.0008	0.0135	0.2548
16 to 24	0.0003	0.0059	0.068
17 to 18	0.0007	0.0082	0.1319
17 to 27	0.0013	0.0173	0.3216
21 to 22	0.0008	0.014	0.2565
22 to 23	0.0006	0.0096	0.1846
23 to 24	0.0022	0.035	0.361
25 to 26	0.0032	0.0323	0.513
26 to 27	0.0014	0.0147	0.2396
26 to 28	0.0043	0.0474	0.7802
26 to 29	0.0057	0.0625	1.029
28 to 29	0.0014	0.0151	0.249

All the details Given in above table are in per unit system at the base voltage of 345KV(Ph-Ph) and 100MVA . Resistance, impedance and suceptance given are for the total

length of transmission lines however HYPERSIM and EMTP will only accept the per Kilometer or per unit length data for the transmission lines. For that reason we need the transmission lines length. We cannot directly assume the length [1]. Phase constant β is practically the same for all transmission lines and this is because of propagation velocity which is somewhat slower than the light velocity (3,00,000 Km/s) i.e $\frac{1}{\sqrt{LC}}$. We calculated the length of each line depending upon the wave propagation velocity and values are given below.

Table 4.2 Transmission line data for HYPERSIM

LINE	Length(Km)	R per Km PU	Reac per Km PU	Suc PER Km PU
1 to 2	133.295	2.62575E-05	0.000308339	0.005241756
1 to 39	108	9.25926E-06	0.000231481	0.006944444
2 to 3	48.97214	2.65457E-05	0.000308339	0.005251966
2 to 25	27.89142	0.000250973	0.000308339	0.005234585
3 to 4	54	2.40741E-05	0.000394444	0.0041
3 to 18	42	2.61905E-05	0.000316667	0.005090476
4 to 5	32	0.000025	0.0004	0.00419375
4 to14	33	2.42424E-05	0.000390909	0.004187879
5 to 6	8.432289	2.37184E-05	0.000308339	0.005146883
5 to8	32	0.000025	0.00035	0.0046125
6 to 7	25	0.000024	0.000368	0.00452
6 to 11	26.59414	2.63216E-05	0.000308339	0.005222955
7 to 8	14.91866	2.68121E-05	0.000308339	0.00522835
8 to 9	93	2.47312E-05	0.000390323	0.004090323
9 to 39	135	7.40741E-06	0.000185185	0.008888889
10 to 11	13.94571	2.86827E-05	0.000308339	0.005227415
10 to 13	13.94571	2.86827E-05	0.000308339	0.005227415
13 to 14	32.7562	2.74757E-05	0.000308339	0.005260073
14 to 15	70.37718	2.55765E-05	0.000308339	0.005200549
15 to 16	31.5	2.85714E-05	0.000298413	0.005428571
16 to 17	27	2.59259E-05	0.00032963	0.00497037
16 to19	60	2.66667E-05	0.000325	0.005066667
16 to 21	46	1.73913E-05	0.000293478	0.00553913
16 to 24	15.5	1.93548E-05	0.000380645	0.004387097
17 to 18	26	2.69231E-05	0.000315385	0.005073077
17 to 27	58	2.24138E-05	0.000298276	0.005544828
21 to 22	47	1.70213E-05	0.000297872	0.005457447
22 to 23	33	1.81818E-05	0.000290909	0.005593939

continued.

Table 4.2 continued.

23 to 24	87	2.52874E-05	0.000402299	0.004149425
25 to 26	100	0.000032	0.000323	0.00513
26 to 27	46	3.04348E-05	0.000319565	0.005208696
26 to 28	150	2.86667E-05	0.000316	0.005201333
26 to 29	200	0.0000285	0.0003125	0.005145
28 to 29	47.5	2.94737E-05	0.000317895	0.005242105

4.3 Transformers

Transformers details for this test system are taken from [N]. Those details consists of R_T (Resistance) and X_T (Reactance) which are equivalent resistance and reactance referred with respect to primary or secondary. For this system we assumed that the values are with respect to primary winding of the transformer. Transformer details are given in the below table.

Table 4.3 Transformers data

BUS	**BUS**	**RESISTANCE(R_T)**	**REACTANCE(X_T)**
30	2	0.0000	0.0181
37	25	0.0006	0.0232
31	6	0.0000	0.0250
32	10	0.0000	0.0200
11	12	0.0016	0.0435
13	12	0.0016	0.0435
34	20	0.0009	0.0180
20	19	0.0007	0.0138
33	19	0.0007	0.0142
36	23	0.0005	0.0272
35	22	0.0000	0.0143
38	29	0.0008	0.0156

All the values in above table are in per unit. For this system transformer at generators primary winding is delta lag with rated voltage of 20KV. Secondary winding is star grounded

with rated voltage of 345KV. All the remaining transformers are grounded stat-star with both the windings rated at 345KV.

But HYPERSIM will ask for individual winding data. As from [46].

$$X_1=X_2/K^2=X_{01}/2 \qquad (4.1)$$

Where K is turns ratio, X_{01} total equivalent reactance and X_1, X_2 are primary, secondary windings individual reactances. Above statement is based on a assumption that the transformers are well designed.

Below table will give all the details regarding transformers for HYPERSIM and EMTP model. All the per unit values of transformers are taken at 100MVA base.

Table 4.4 Transformers data for HYPERSIM

BUS	BUS	Primary Rated Voltage KV	Seco Rated Voltage KV	Pri Conne Type	Sec Conne type	Pri Resista Pu	Sec Resista Pu	Pri Reacta Pu	Sec Reacta Pu
30	2	20	345	Delta- lag	Star	0.0000	0.00905	0.0000	0.00905
37	25	20	345	Delta- lag	Star	0.0003	0.0116	0.0003	0.0116
31	6	20	345	Delta- lag	Star	0.0000	0.0125	0.0000	0.0125
32	10	20	345	Delta- lag	Star	0.0000	0.0100	0.0000	0.0100
11	12	345	345	Star	Star	0.0008	0.02175	0.0008	0.02175
13	12	345	345	Star	Star	0.0008	0.02175	0.0008	0.02175
34	20	20	345	Delta- lag	Star	0.00045	0.0090	0.00045	0.0090
20	19	345	345	Star	Star	0.00035	0.0069	0.00035	0.0069
33	19	20	345	Delta- lag	Star	0.00035	0.0071	0.00035	0.0071
36	23	20	345	Delta- lag	Star	0.00025	0.0136	0.00025	0.0136
35	22	20	345	Delta- lag	Star	0.0000	0.00715	0.0000	0.00715
38	29	20	345	Delta- lag	Star	0.0004	0.0078	0.0004	0.0078

4.4 Generators

IEEE 39BUS system has 10 generators at different buses which were already mentioned. Out of those 10 generators a generator at BUS 31 which is named as GEN2 is assumed as a slack bus generator. Except BUS31 all the buses numbered as 30 to 39 are called as PV buses because of the generators connected at those buses. All the remaining buses are called as PQ buses. The bus which is considered as slack bus has a voltage angle as zero because all the remaining voltage angles are measured with respect to the slack generator. The generator which is considered as slack generator will give all the deficient power in the network and it also gives the power required to cover the losses.

Below table gives the information regarding initial load flow conditions for IEEE 39 BUS 10 generators. All the values are in 100-MVA power base and machines rated terminal voltage.

Table 4.5: Generators initial load flow details

BUS	GENERATOR	RATED VOLTAGE KV	VOLTAGE Pu	ACTIVE POWER Pu
30	10	20	1.0475	2.50
31	2	20	0.9820	Slack Generator
32	3	20	0.9831	6.50
33	4	20	0.9972	6.32
34	5	20	1.0123	5.08
35	6	20	1.0493	6.50
36	7	20	1.0635	5.60
37	8	20	1.0278	5.40
38	9	20	1.0265	8.30
39	1	345	1.0300	10.0

Below table will give the information about all the generators rated voltage, inertia, resistance, leakage reactance and transient - sub transient reactance's and time constants.

Table 4.6: Generator details

GEN	R_a	X_l	X_d	X_q	$X_d^{\|}$	$X_q^{\|}$	$X_d^{\|\|}$	$X_q^{\|\|}$	$T_{d0}^{\|}$	$T_{q0}^{\|}$	$T_{d0}^{\|\|}$	$T_{q0}^{\|\|}$	H(S)
1	0	0.003	0.2	0.019	0.006	0.008	0.0006	0.0006	7	0.7	0.033	0.0563	500
2	0	0.035	0.295	0.282	0.0697	0.17	0.0369	0.0369	6.56	1.5	0.066	0.066	30.3
3	0	0.0304	0.2495	0.237	0.0531	0.0876	0.032	0.032	5.7	1.5	0.057	0.057	35.8
4	0	0.0295	0.262	0.258	0.0436	0.166	0.031	0.031	5.69	1.5	0.057	0.057	28.6
5	0	0.054	0.67	0.62	0.132	0.166	0.0568	0.0568	5.4	0.44	0.054	0.054	26
6	0	0.0224	0.254	0.241	0.05	0.0814	0.0236	0.0236	7.3	0.4	0.073	0.073	34.8
7	0	0.0322	0.295	0.292	0.049	0.186	0.034	0.034	5.66	1.5	0.056	0.056	26.4
8	0	0.028	0.29	0.28	0.057	0.0911	0.03	0.03	6.7	0.41	0.067	0.067	24.3
9	0	0.0298	0.2106	0.205	0.057	0.0587	0.0314	0.0314	4.79	1.96	0.047	0.047	34.5
10	0	0.0125	0.1	0.069	0.031	0.018	0.0132	0.0132	10.2	0.3	0.1	0.1	42

4.5 Excitation System

The detailed model of excitation system for generator was already discussed in the chapter 3 of this thesis report. Following table will give the required values for the excitation model of the generator. All the values are rated with respect to their particular machines ratings. For all the excitation systems values of feedback transfer function are considered as zero that is feedback time constant T_f and feedback gain K_f are zeros. This means literally no feed back in the excitation system. Some of the values in the following table are assumed values.

Table 4.7: Generators Excitation system details

GEN	Ex_Tr(s)	Ex_Ka	Ex_ta(s)	Ex_Kp	Ex_Vtmin Pu	Ex_Vtmax Pu	Ex_Vrmin Pu	Ex_Vrmax Pu
1	0.01	125	0.001	5.3	0.1	100	-5.7	12.3
2	0.01	125	0.001	5.3	0.1	100	-5.7	12.3
3	0.01	125	0.001	10	0.1	100	-5.7	12.3
4	0.01	125	0.001	10	0.1	100	-5.7	12.3
5	0.01	125	0.001	20	0.1	100	-5.7	12.3

continued.

Table 4.7 continued.

6	0.01	125	0.001	10	0.1	100	-5.7	12.3
7	0.01	125	0.001	15	0.1	100	-5.7	12.3
8	0.01	125	0.001	15	0.1	100	-5.7	12.3
9	0.01	125	0.001	10	0.1	100	-5.7	12.3
10	0.01	125	0.001	10	0.1	100	-5.7	12.3

4.6 Loads

Dynamic load model considered in this thesis was already discussed in the chapter 3 of this report. IEEE 39BUS system has total 19 loads which are connected at different buses. Below table have the values of all 19 loads.

Table 4.8: Load data

BUS	**Rated Volatge KV**	**Load MW**	**Load MVAR**
3	345	322	2.40
4	345	500	184
7	345	233.8	84.0
8	345	522	176.0
12	345	7.5	88.0
15	345	320	153.0
16	345	329	32.3
18	345	158	30.0
20	345	628	103.0
21	345	274	115.0
23	345	247.5	84.6
24	345	308.6	-92.2
25	345	224	47.2
26	345	139	17.0
27	345	281	75.5
28	345	206	27.6
29	345	283.5	26.9
31	20	9.2	4.6
39	345	1104	250

Chapter 5

Simulation Results

5.1 Real time Simulations

To test the proposed method in distinguishing voltage stability ahead of time for IEEE39 bus equivalent test system was built in Hypersim with the thermal generators and dynamic loads in it to simulate voltage stable and unstable cases. At first ULTCs were not included in the system. The screen shot of IEEE39 bus system in hypersim is shown in below figure.

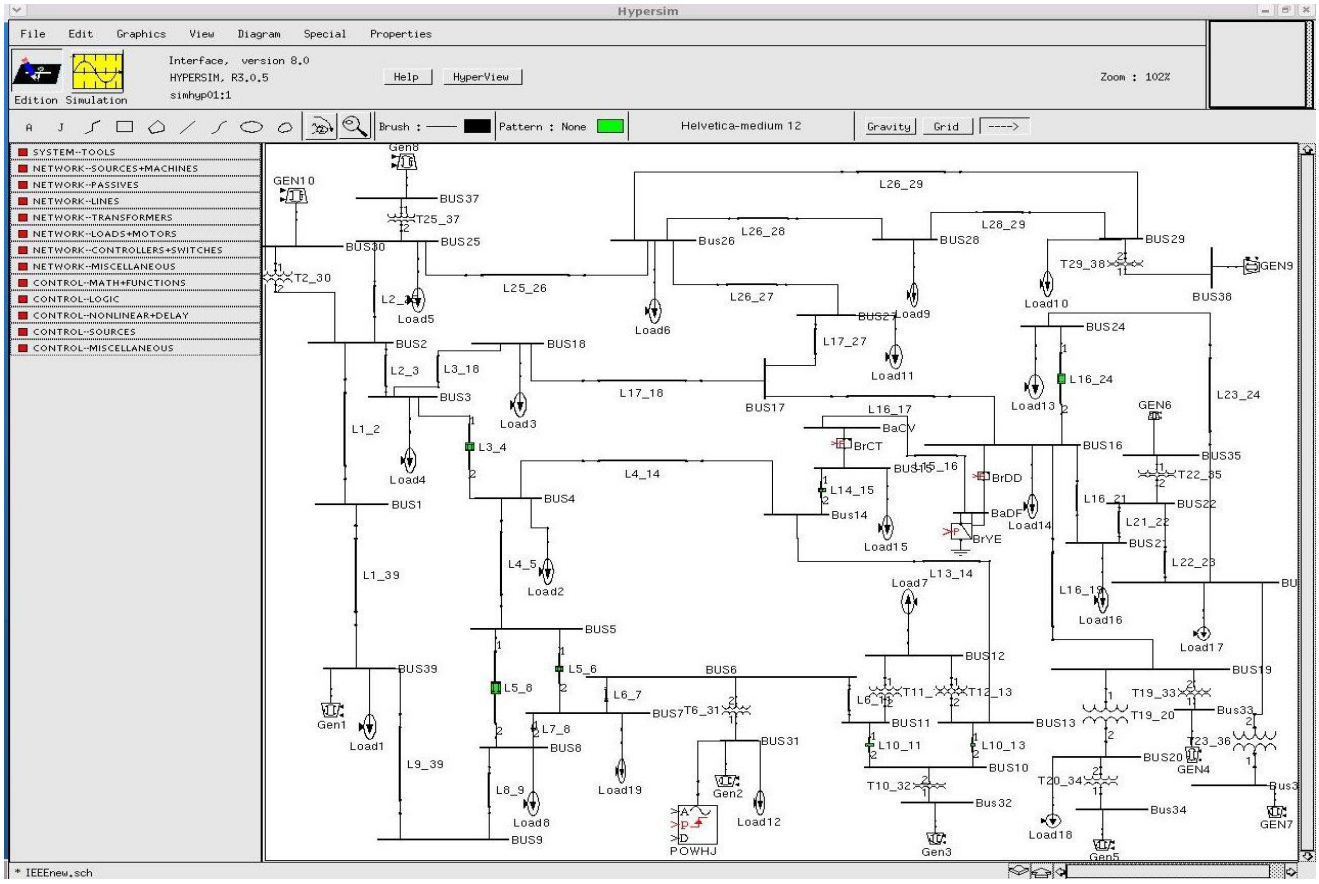

Figure 5.1 IEEE39 Bus equivalent System in Hypersim

Load flow solution of the IEEE39 bus system was verified with the other sources. After getting a desired load flow solution replaced the regular transformers with ULTCs to include all types of dynamics and to replicate the real world power system problems. After replacing the reguler transformers with ULTCs, real time simulations in HYPERSIM were not successful. Because of those problems replaced the transformers with the ULTCs one by one and figured out that by inserting more than two ULTCs in to the system simulations were unsuccessful with HYPERSIM. The main reasons causing these problems is number of processors available for simulations. We only have 12 processors SGI machine to do real time simulations in HYPERSIM. Because of this the same system is built in EMTP software and it is shown below.

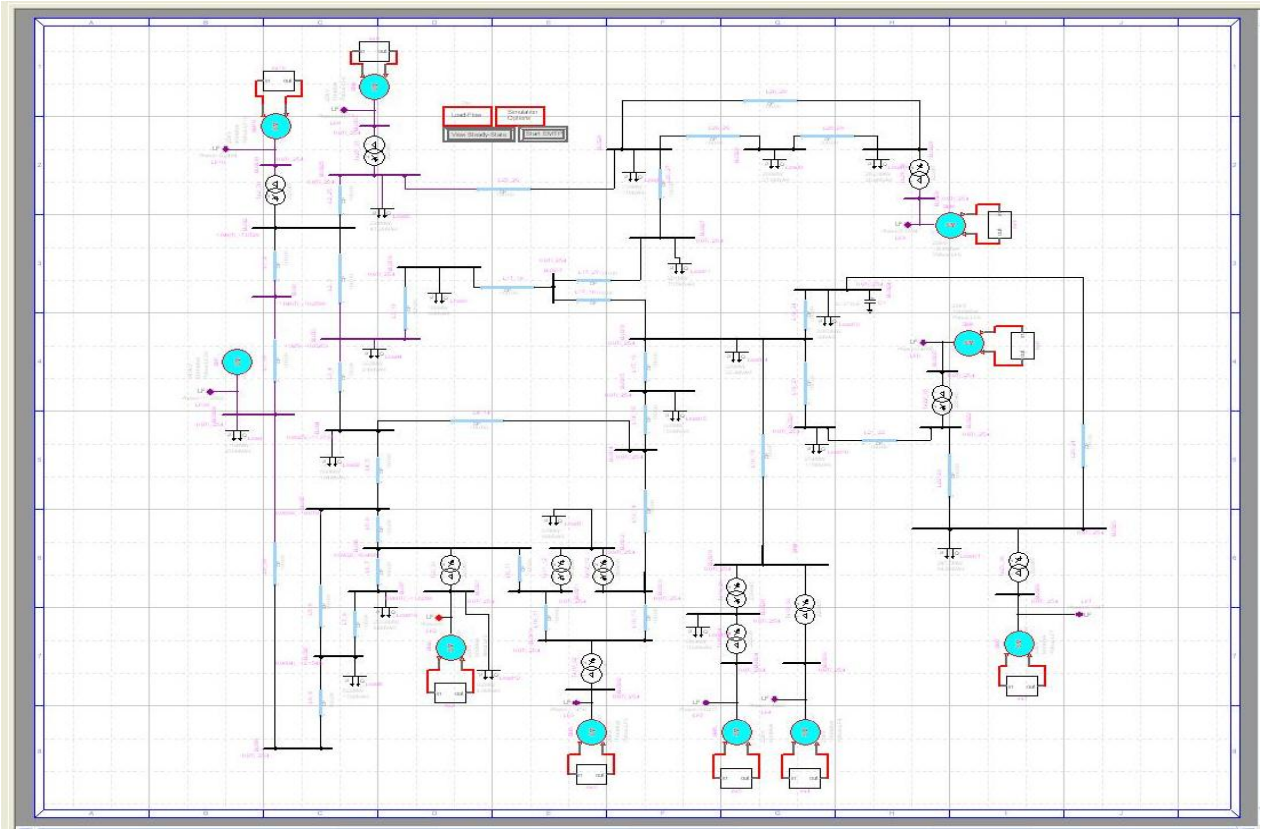

Figure 5.2 IEEE39 Bus equivalent System in EMTP

After building the IEEE 39 bus system in EMTP load flow solution is matched with HYPERSIM and other sources.

A small area is choosed in the 39-bus system and concentrated on that area to prove our statement regarding detection of blackouts using real time simulators or transients simulator and pattern recognition techniques. Snapshots of the chosen area in IEEE39 bus system is shown below.

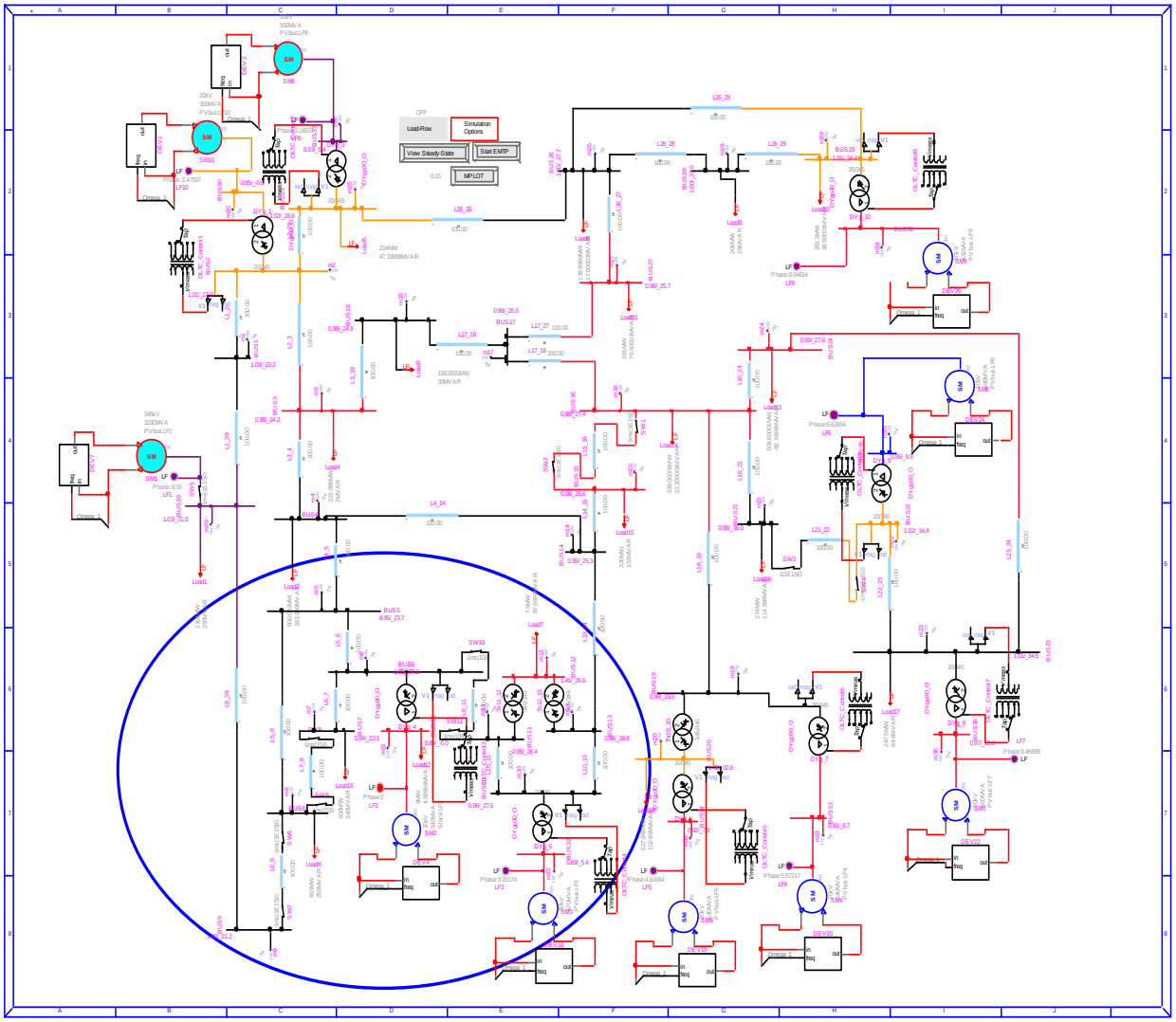

Figure 5.3 A small area choosed for transient simulations in EMTP

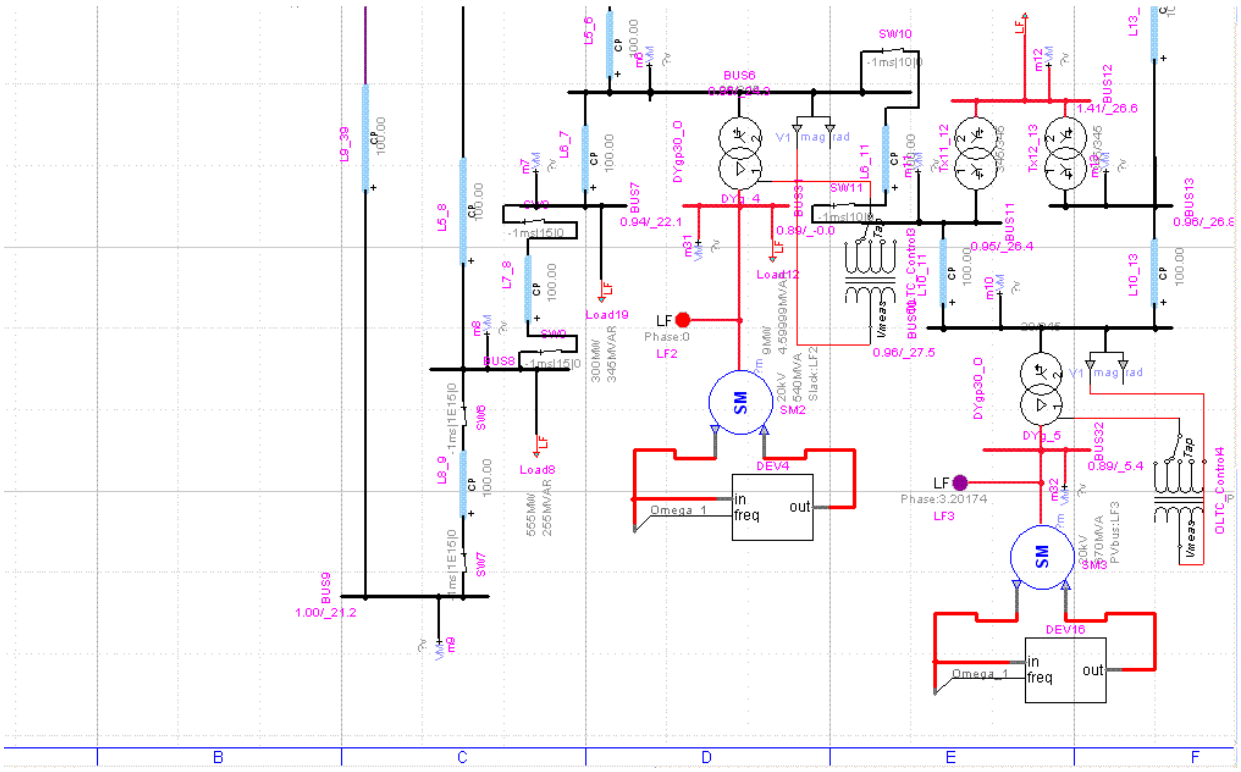

Figure 5.4 Zoomed in Figure 5.3

Time domain Simulations are carried out for several cases by applying different contingencies and different loading conditions on the chosen area and distinguished the stable and unstable cases by observing the voltage waveforms at all the buses. Those cases are given in below table and captured voltage wave forms for these cases are shown later in this chapter. Table 5.1 has the real and reactive power loads connected at the particular mentioned bus, the type of contingency applied and voltage stability for each case.

Table 5.1 Loads applied and contingency applied for each training case

Case	Bus Number	P(MW)	Q(MW)	Contingency	Stable/Unstable
1	7	270	240	L7_8	Stable
2	7	270	240	L6_11	Stable
3	7	233.8(Base Case)	84(Base Case)	L6_11	Stable
4	7	233.8(Base Case)	84(Base Case)	L8_9	Stable
5	8	600	210	L8_9	Stable
6	7	330	360	L6_11	Unstable

continued.

Table 5.1 continued.

7	7	330	360	L8_9	Unstable
8	7	300	150	L8_9	Unstable
	8	600	360		
	12	60	150		
9	7	300	345	L6_7	Unstable
	8	555	255		
10	7	330	360	L7_8	Unstable

The waveform of selected Bus 7 voltage for case 4 are presented in Figures5.5-5.6 . Transmission line between Bus 8 and Bus 9 was disconnected at 10 seconds. Now the power required by load 8 has to be supplied by SM2 and SM3 through the transmission line L7_8. This causes voltage drop at the terminal buses of the machines SM2 and SM3.When the line was disconnected, voltage at Bus 7 drops from 0.94 p.u to 0.91 p.u. The time constant for all the ULTCs (Under load tap changers) is 20 seconds. Around 32 seconds ULTC3 near the synchronous machine SM2 operates and try to increase the voltage at the buses close to SM2 especially at Bus 6 where the ULTC3 was connected. At 50 seconds ULTC near the machine SM3 operates and increases the voltage at Bus 10 where ULTC4 was connected. This intern increase the voltage at the Bus 6, Bus 7 and Bus 8. These two ULTCS will bring the voltage at Bus 6 and Bus 10 to their prefault voltages, but Bus 8 voltage was not came back to its prefault voltage because the power required by Load 8 is now solly supplied by L7_8 which will lead to more voltage drop in the transmission line. The post fault voltage is settled at 0.93 p.u. By looking at the Bus 7 voltage will confirm that the system is voltage stable. This can be observed in below figures.

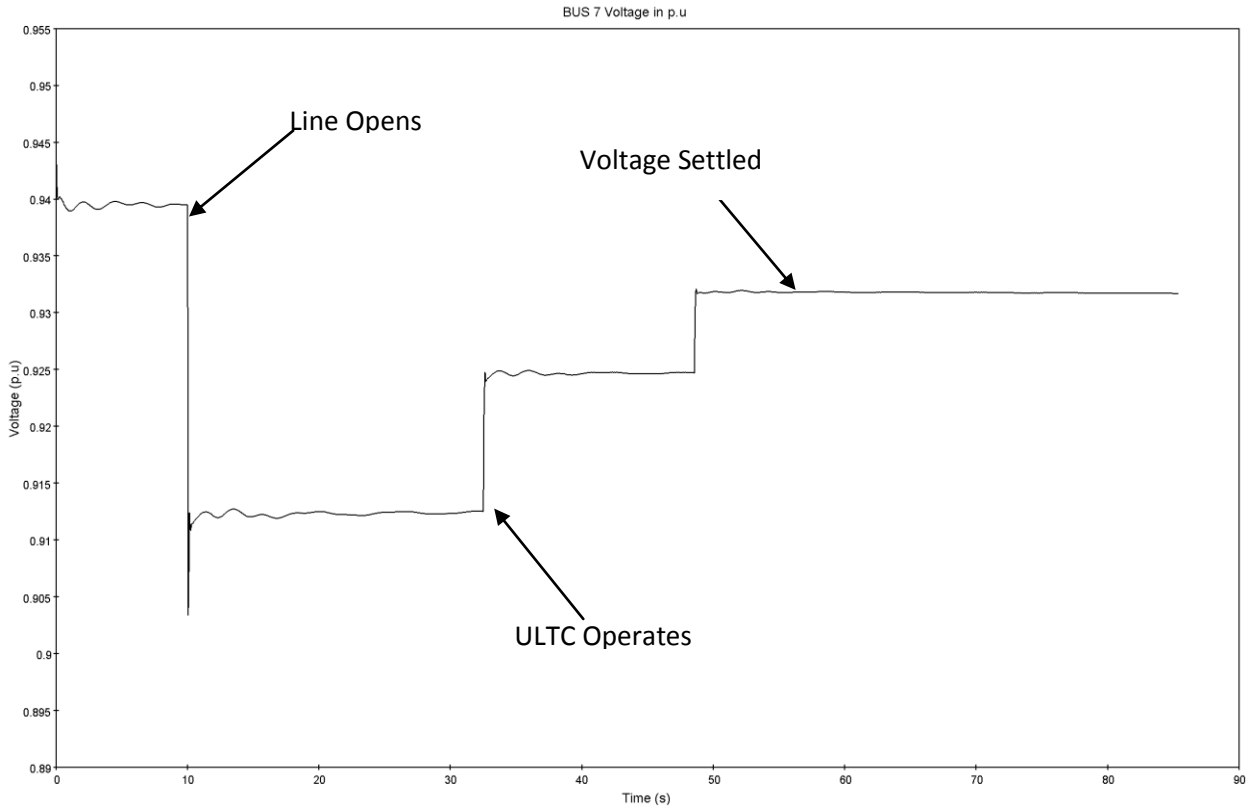

Figure 5.5 Bus 7 voltage for stable case 4

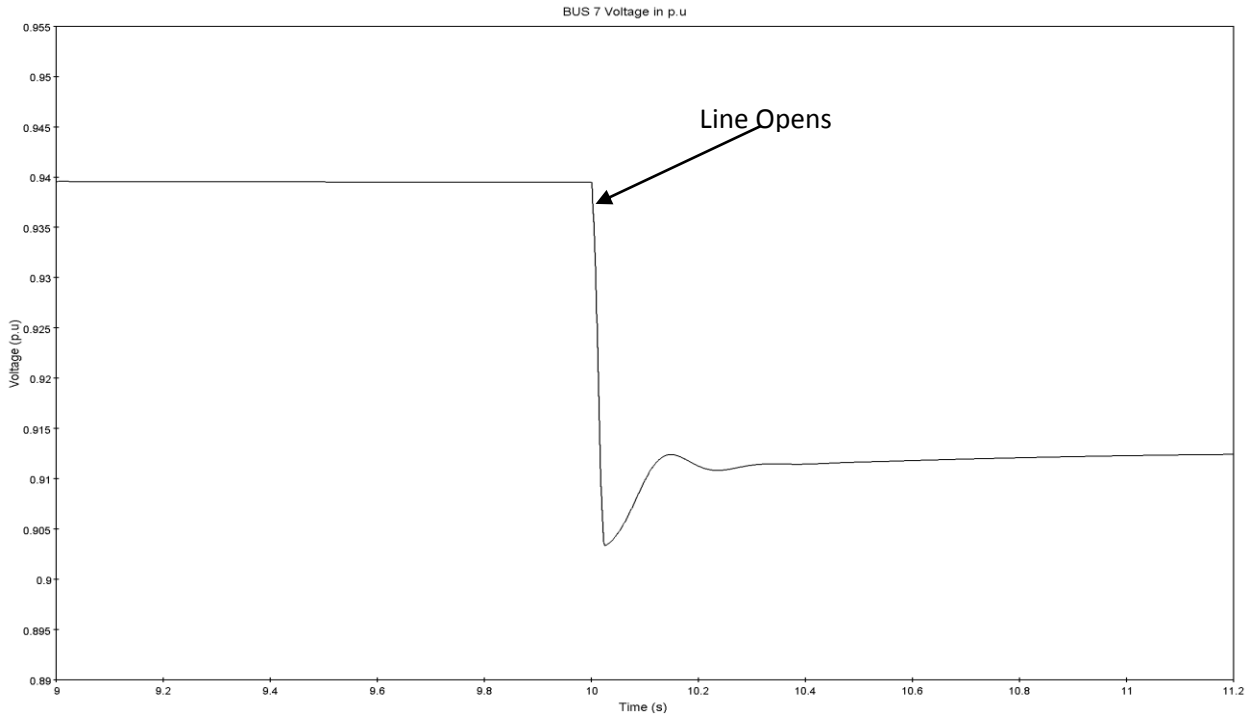

Figure 5.6 Zoomed in Figure 5.5

Figure 5.7- 5.8 illustrates the simulation result for an outage of transmission line at 10 seconds between Bus 8 and Bus 9 for case 7 loading. Power required by load 8 has to be supplied by SM2 and SM3 through the transmission line L7_8. This causes voltage drop at the terminal buses of the machines SM2 and SM3. After the tripping of transmission line reactive power required by load at Bus 8 is taking power from SM2 and SM3 which is given by over exciting the synchronous machines. Time constant of VOX (Over Excitation limiter) is set to 20 seconds. These over excitation limiters will try to control the excitation current to synchronous machines. This causes SM2 and SM3 to deliver constant reactive power because reactive power and voltage are relative to each other. This means supplying more reactive power to load is achieved by increasing the excitation current which will increase the terminal voltage of synchronous machines. But when ULTC detects an under voltage, it will try to increase the voltage on the secondary of the transformer by changing the tap position. This will decrease the voltage on the primary side of transformer which is connected to the synchronous machines terminal Bus. Then generators cannot give enough reactive power to load. The net effect of each tap movement of ULTC is to reduce the secondary voltage rather than increase. The combined action of VOX and ULTC will lead to voltage collapse and it is shown in below figure.

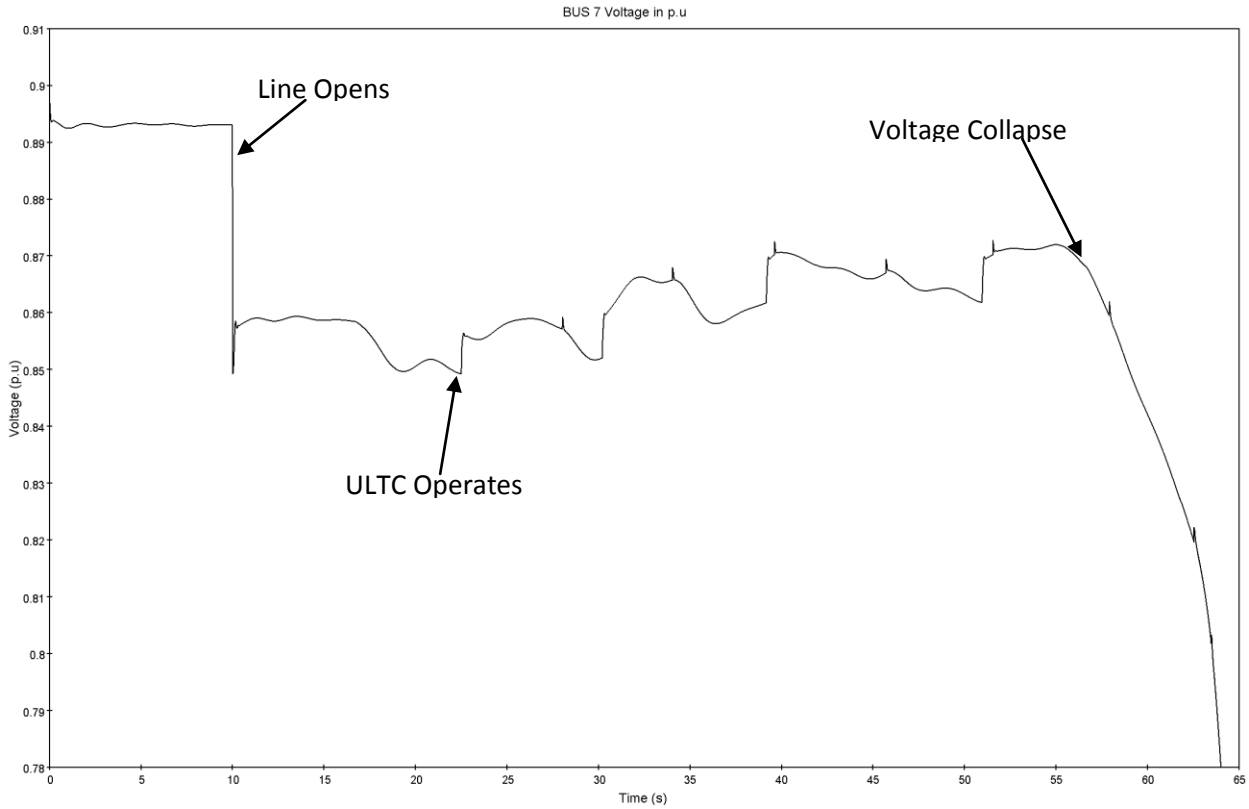

Figure 5.7 Bus 7 voltage for unstable case 7

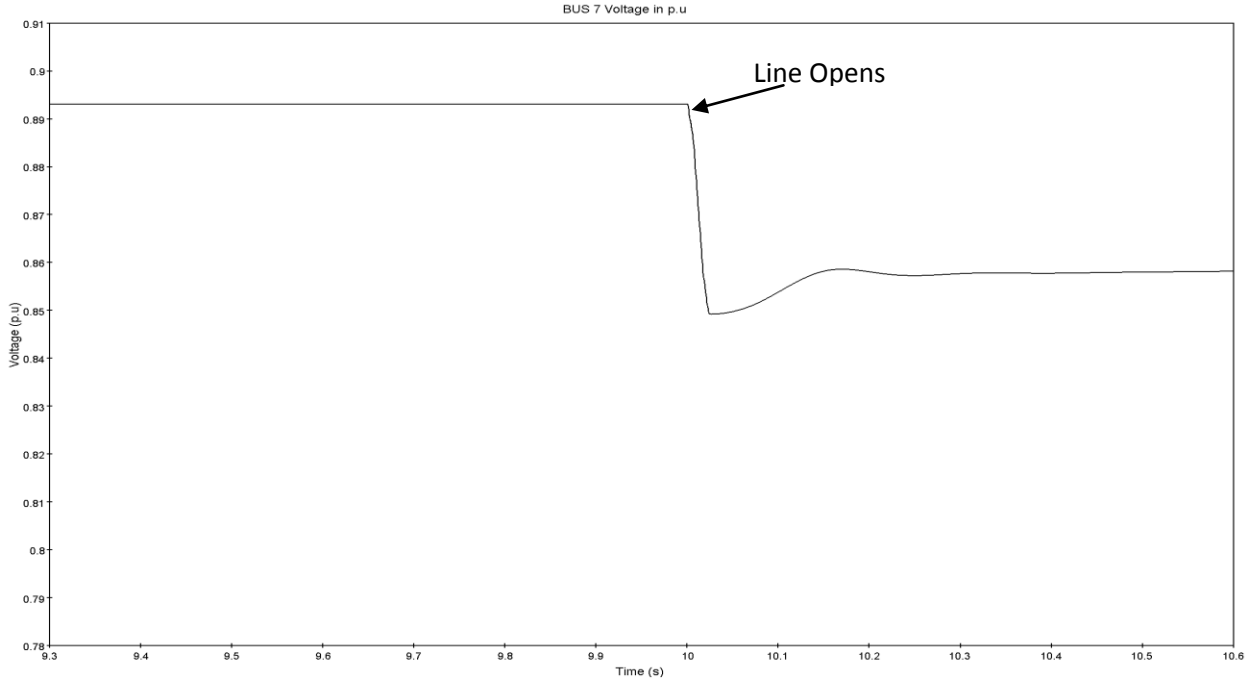

Figure 5.8 Zoomed in Figure 5.7

Transient simulations for all the remaining cases are shown at the end of this chapter. The first 15 seconds of the simulations are studied to distinguish voltage stability problem from transient stability. The first 15 seconds includes the disconnecting of the transmission line at 10 seconds and the transients after disconnecting the transmission line. These are sufficient data to detect voltage stability from transient stability.

5.2 Regularized Least-Square Method

The 10 transient simulation cases of 15 seconds duration were used to train the regularized least-squares classification algorithm. Then 4 other transient simulation cases were simulated to test the proposed method in detecting voltage collapse from transient stability. All these 14 cases were simulated in EMTP software and the stability is known in advance for these cases. The four test cases proposed are shown in below table and the voltage waveforms for these four test cases are shown at the end of the chapter 5. In the last stage of the proposed technique we will take the four test cases as inputs in to the trained pattern recognition algorithm and use the model to predict the stability of the test cases. After comparing the results from the trained algorithm it is proved that the algorithm is well trained and is 100% accurate in predicting voltage collapse from transient stability.

Table 5.2 Loads applied and contingencies for test cases

Case	Bus Number	P(MW)	Q(MW)	Contingency	Observed Stability from EMTP	RLSC Predicted Stability
Test 1	7	233.8(Base	84(Base Case)	L7_8	Stable	Stable
Test 2	7	330	360	L7_8	Unstable	Unstable
Test 3	8	600	210	L6_11	Stable	Stable
Test 4	7	300	345	L8_9	Unstable	Unstable
	8	555	255			

As seen from the last two columns of Table 5.2, the RLSC accurately predicted all four simulated cases.

Figure 5.9 represents Bus 7 voltage for stable case 1 of Table 5.1. The transmission line was disconnected at 10 seconds, ULTCs operated with some time delay to restore voltage to precontingency value and at last voltage settled around 40 seconds. Figure 5.10 is zoomed in figure of Figure 5.9 around 10 seconds where the transmission line was disconnected.

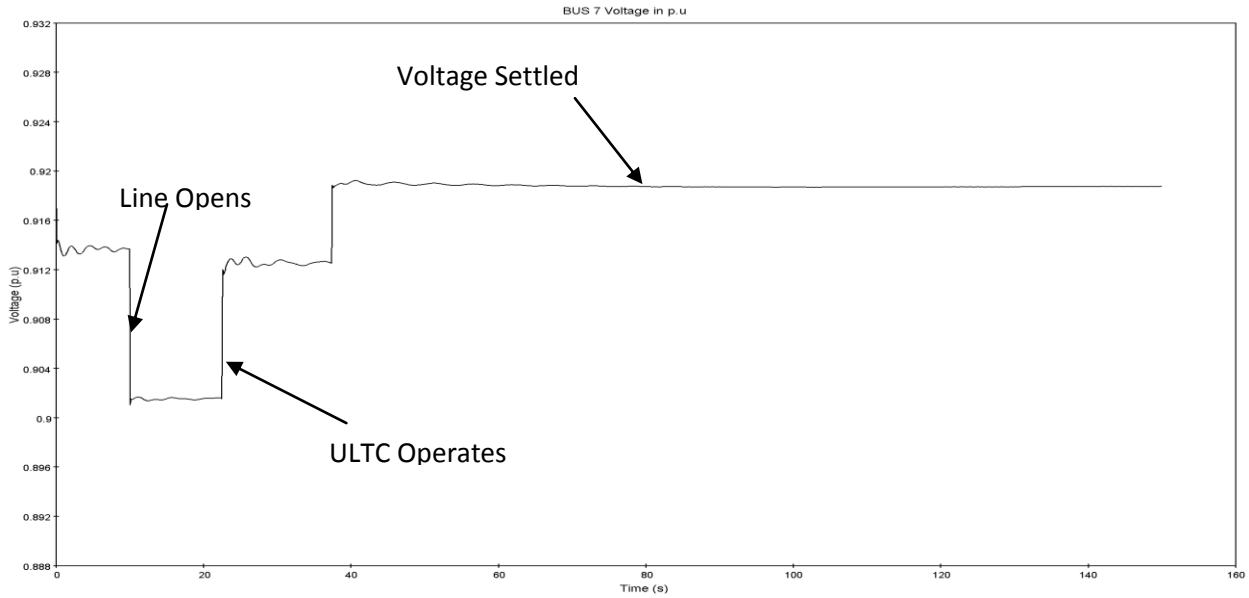

Figure 5.9 Bus 7 voltage for stable case 1

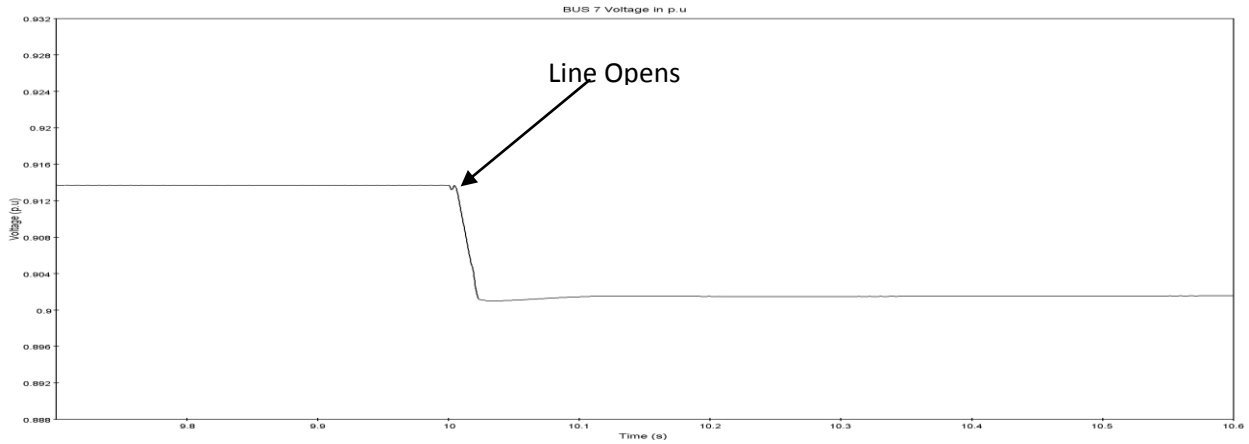

Figure 5.10 Zoomed in Figure 5.9

Figure 5.11 represents Bus 7 voltage for stable case 2 of Table 5.1. The transmission line was disconnected at 10 seconds, ULTCs operated with some time delay to restore voltage to precontingency value and at last voltage settled around 50 seconds. Figure 5.12 is zoomed in figure of Figure 5.11 around 10 seconds where the transmission line was disconnected.

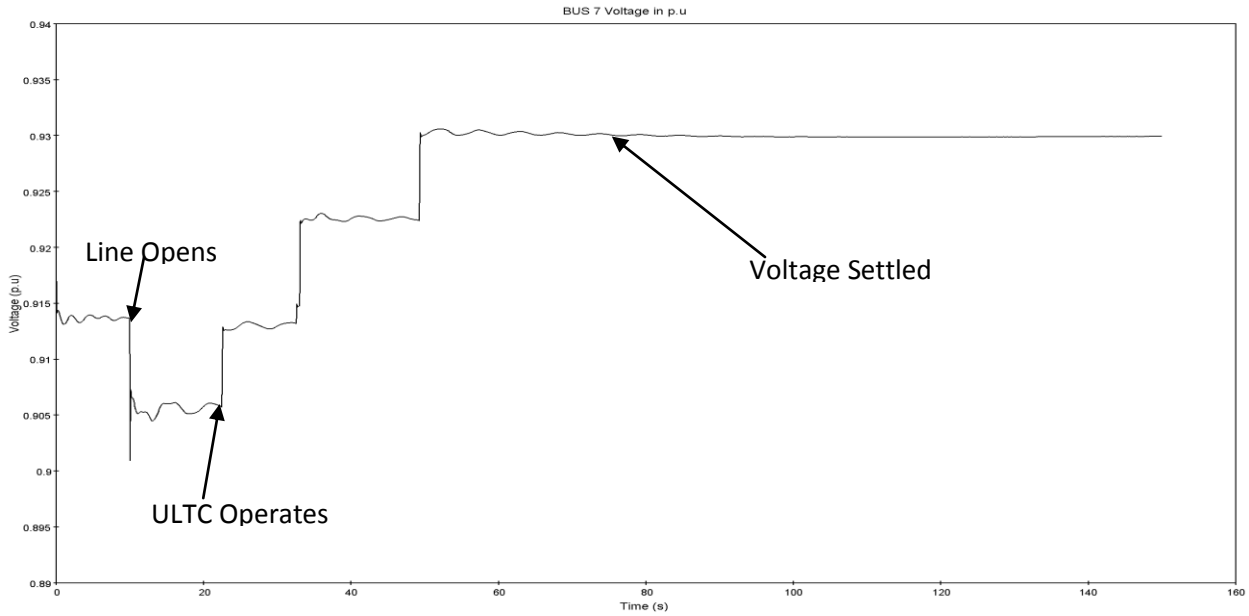

Figure 5.11 Bus 7 voltage for stable case 2

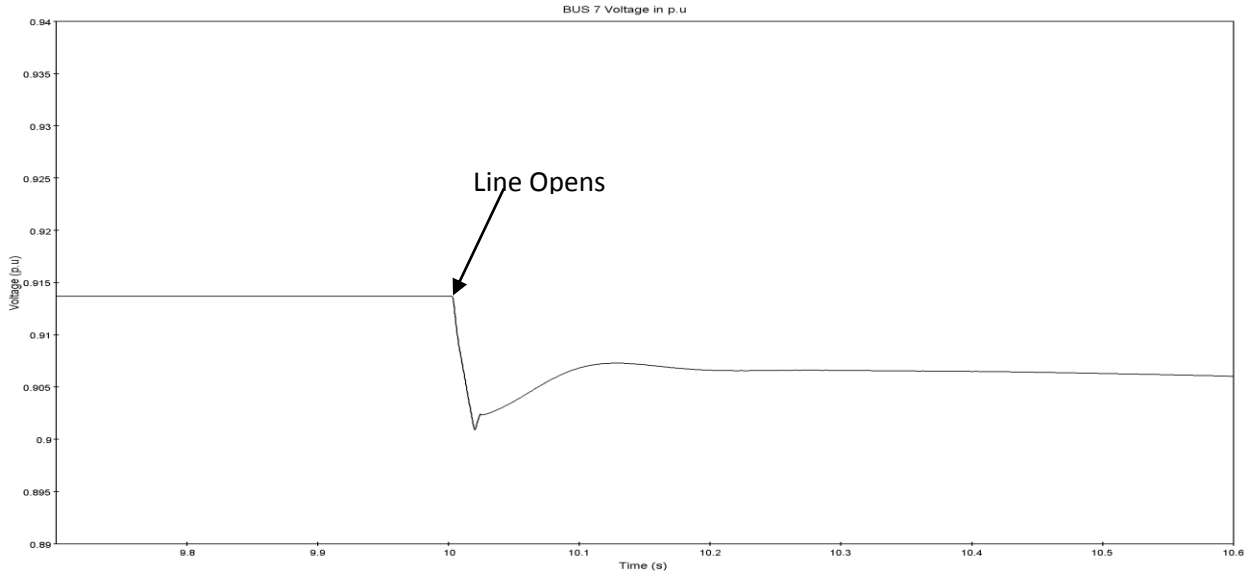

Figure 5.12 Zoomed in Figure 5.11

Figure 5.13 represents Bus 7 voltage for stable case 3 of Table 5.1. The transmission line was disconnected at 10 seconds, ULTCs operated with some time delay to restore voltage to precontingency value and at last voltage settled around 20 seconds. Figure 5.14 is zoomed in figure of Figure 5.13 around 10 seconds where the transmission line was disconnected.

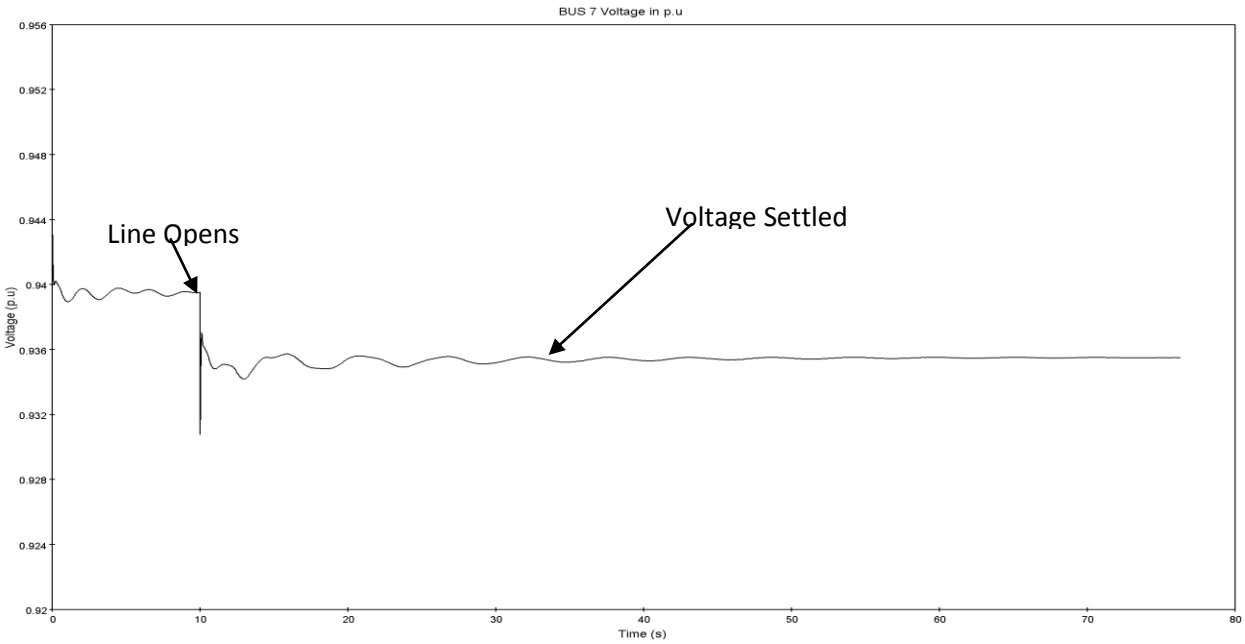

Figure 5.13 Bus 7 voltage for stable case 3

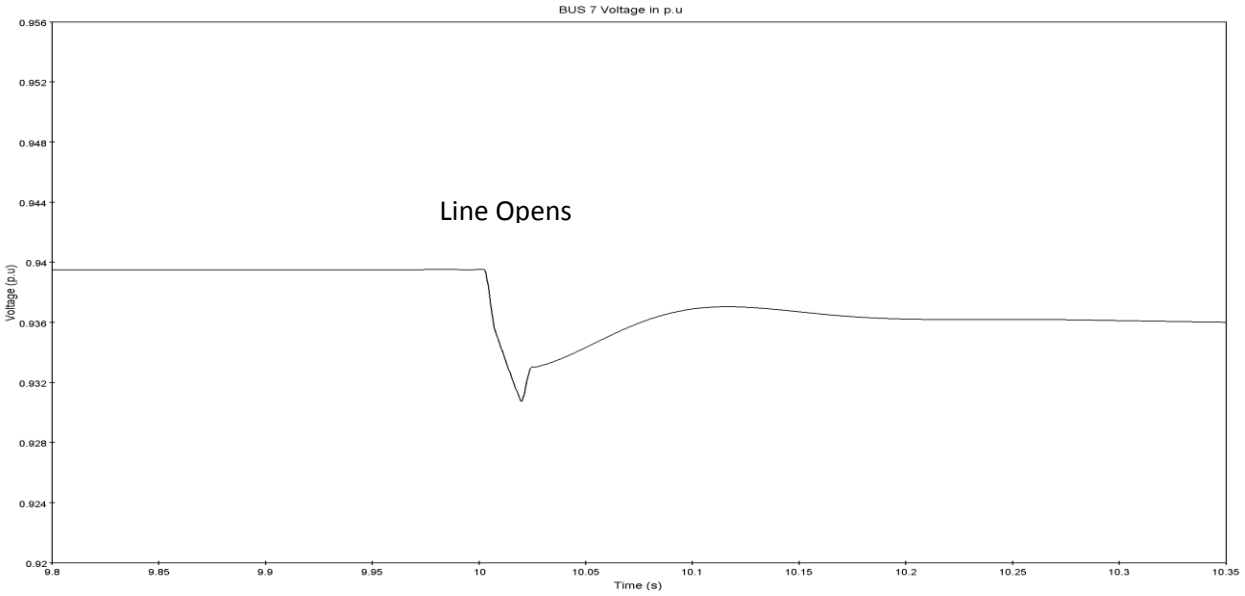

Figure 5.14 Zoomed in Figure5.13

Figure 5.15 represents Bus 7 voltage for stable case 5 of Table 5.1. The transmission line was disconnected at 10 seconds, ULTCs operated with some time delay to restore voltage to precontingency value and at last voltage settled around 45 seconds. Figure 5.16 is zoomed in figure of Figure 5.15 around 10 seconds where the transmission line was disconnected.

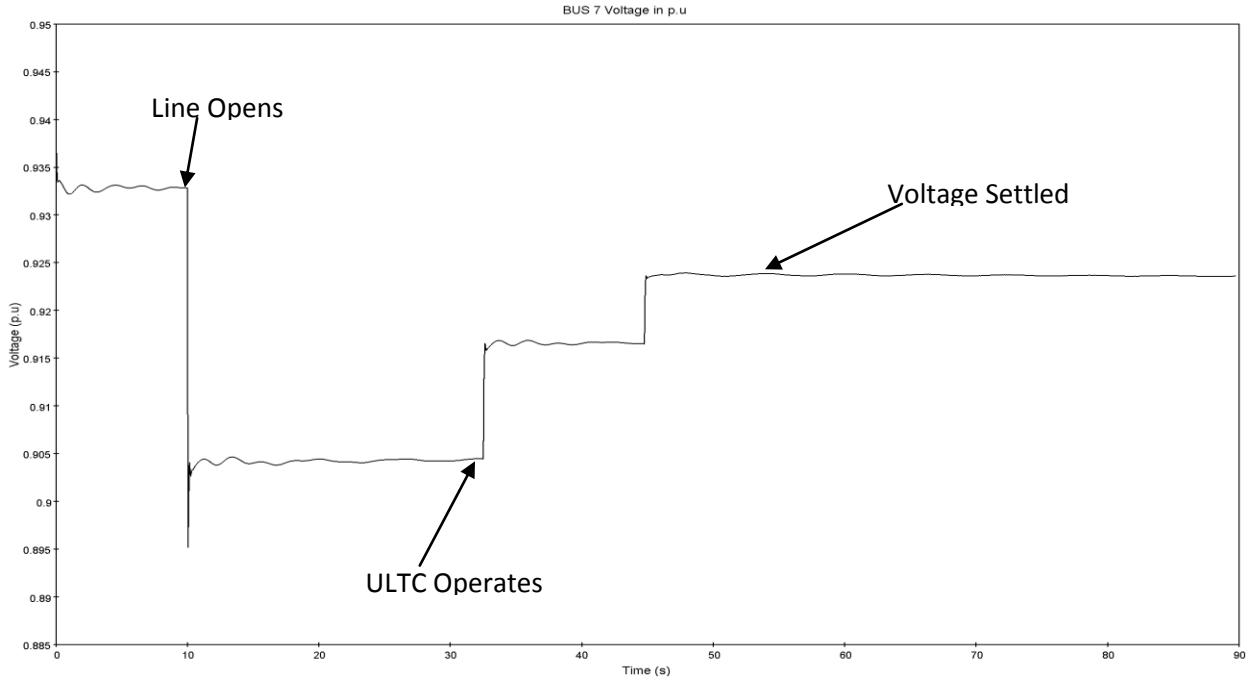

Figure 5.15 Bus 7 voltage for stable case 5

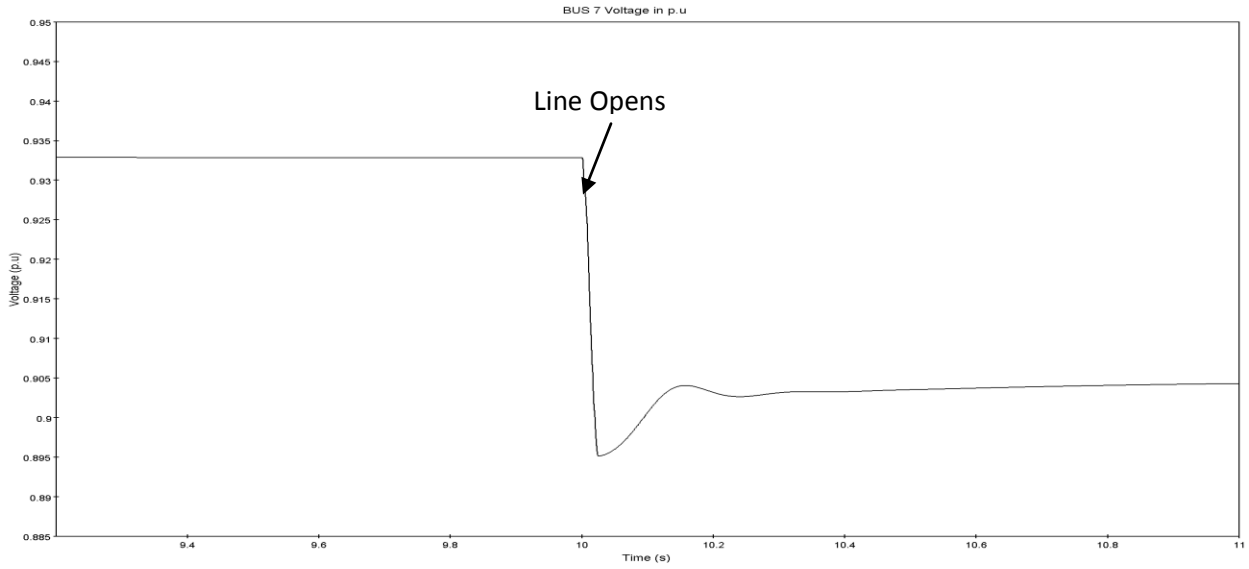

Figure 5.16 Zoomed in Figure 5.15

Figure 5.17 represents Bus 7 voltage for unstable case 6 of Table 5.1. The transmission line was disconnected at 10 seconds, ULTCs operated with some time delay to restore voltage to precontingency value and at last voltage collapsed around 55 seconds. Figure 5.18 is zoomed in figure of Figure 5.17 around 10 seconds where the transmission line was disconnected.

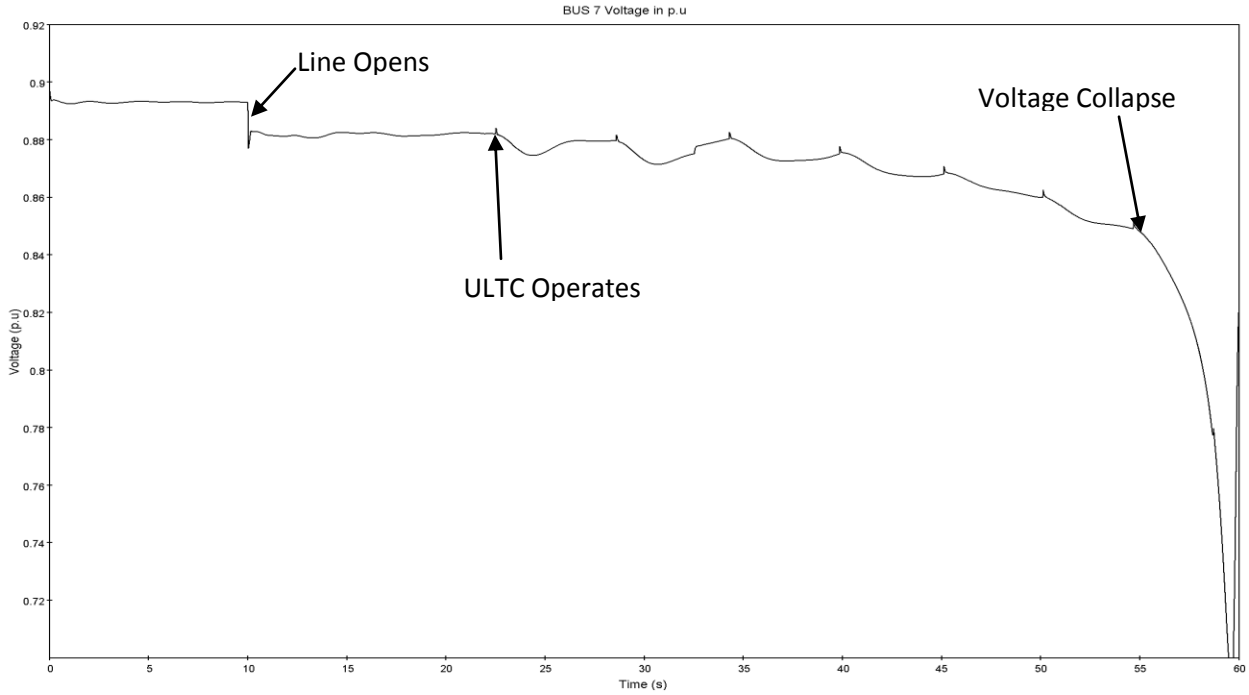

Figure 5.17 Bus 7 voltage for unstable case 6

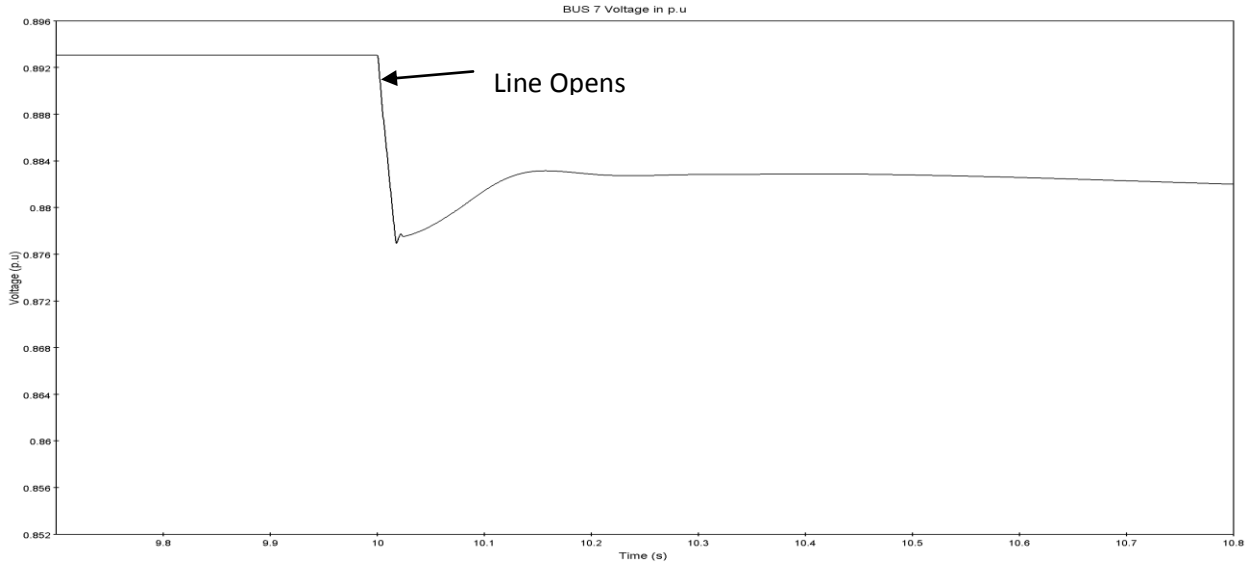

Figure 5.18 Zoomed in Figure5.17

Figure 5.19 represents Bus 7 voltage for unstable case 8 of Table 5.1. The transmission line was disconnected at 10 seconds, ULTCs operated with some time delay to restore voltage to precontingency value and at last voltage collapsed around 45 seconds. Figure 5.20 is zoomed in figure of Figure 5.19 around 10 seconds where the transmission line was disconnected.

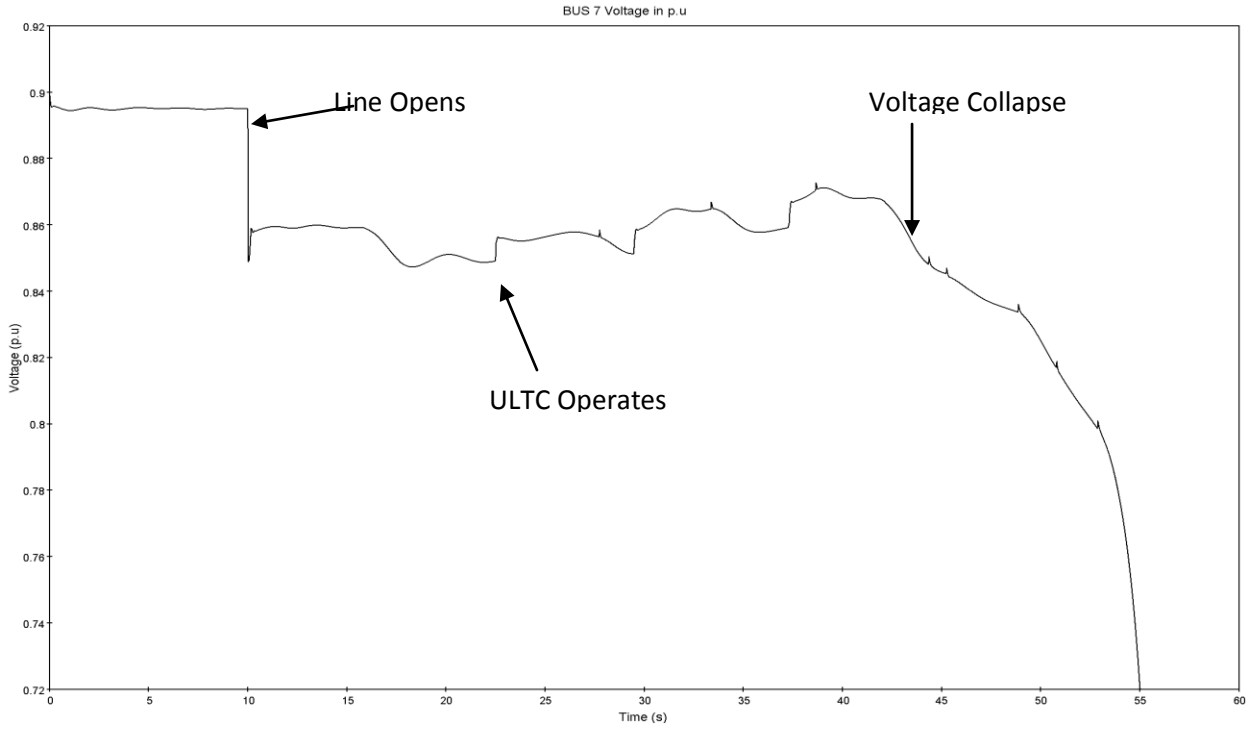

Figure 5.19 Bus 7 voltage for unstable case 8

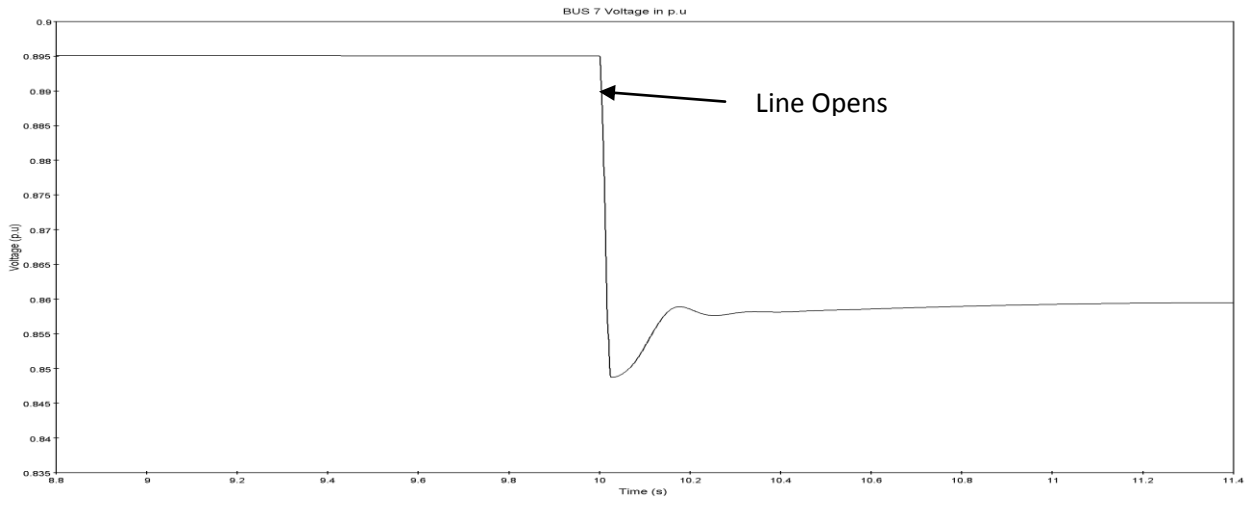

Figure 5.20 Zoomed in Figure 5.19

Figure 5.21 represents Bus 7 voltage for unstable case 9 of Table 5.1. The transmission line was disconnected at 10 seconds, ULTCs operated with some time delay to restore voltage to precontingency value and at last voltage collapsed around 100 seconds. Figure 5.22 is zoomed in figure of Figure 5.21 around 10 seconds where the transmission line was disconnected.

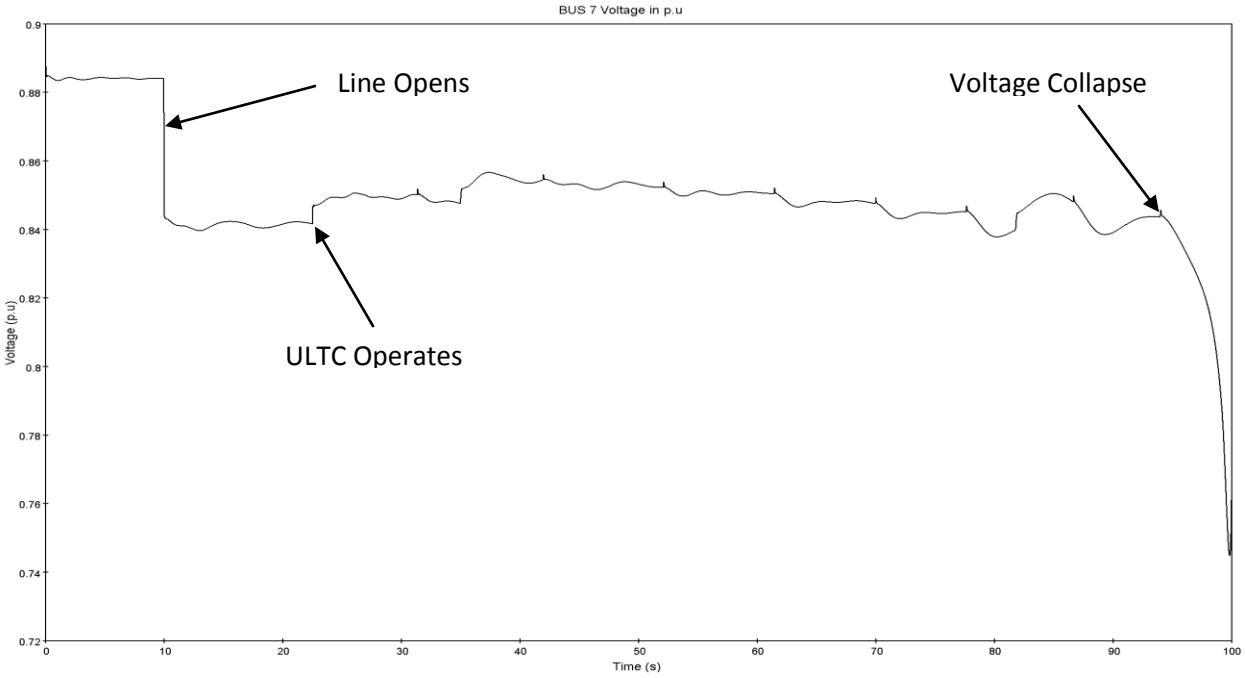

Figure 5.21 Bus 7 voltage for unstable case 9

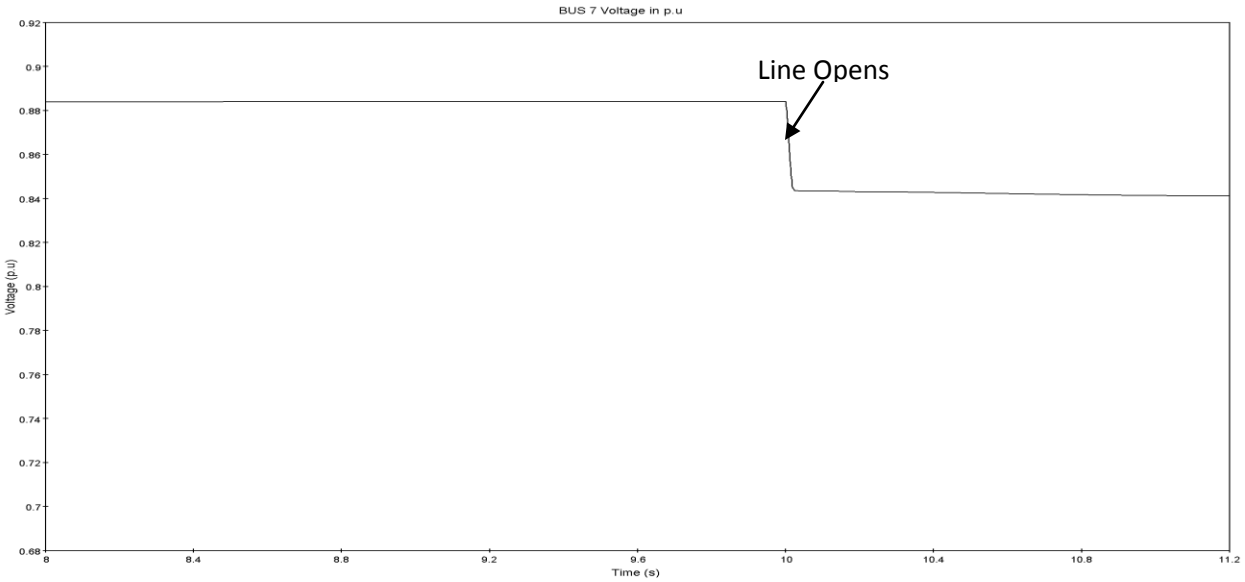

Figure 5.22 Zoomed in Figure 5.21

Figure 5.23 represents Bus 7 voltage for unstable case 10 of Table 5.1. The transmission line was disconnected at 10 seconds, ULTCs operated with some time delay to restore voltage to precontingency value and at last voltage collapsed around 95 seconds. Figure 5.24 is zoomed in figure of Figure 5.22 around 10 seconds where the transmission line was disconnected.

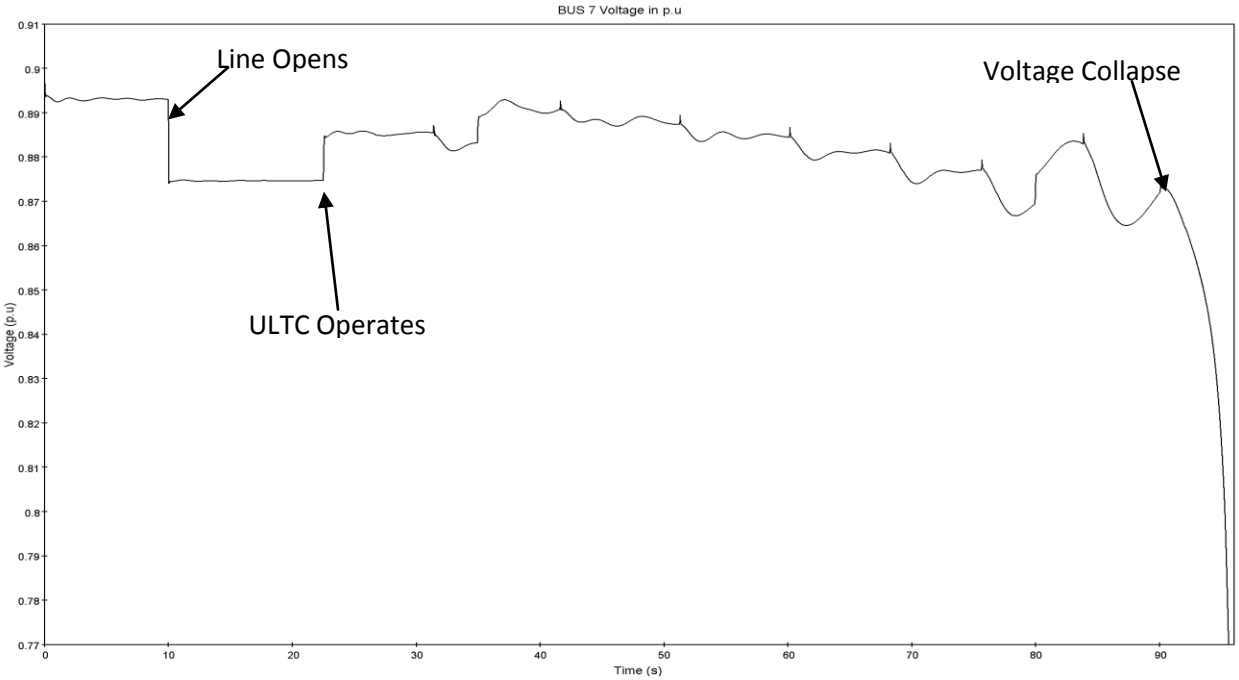

Figure 5.23 Bus 7 voltage for unstable case 10

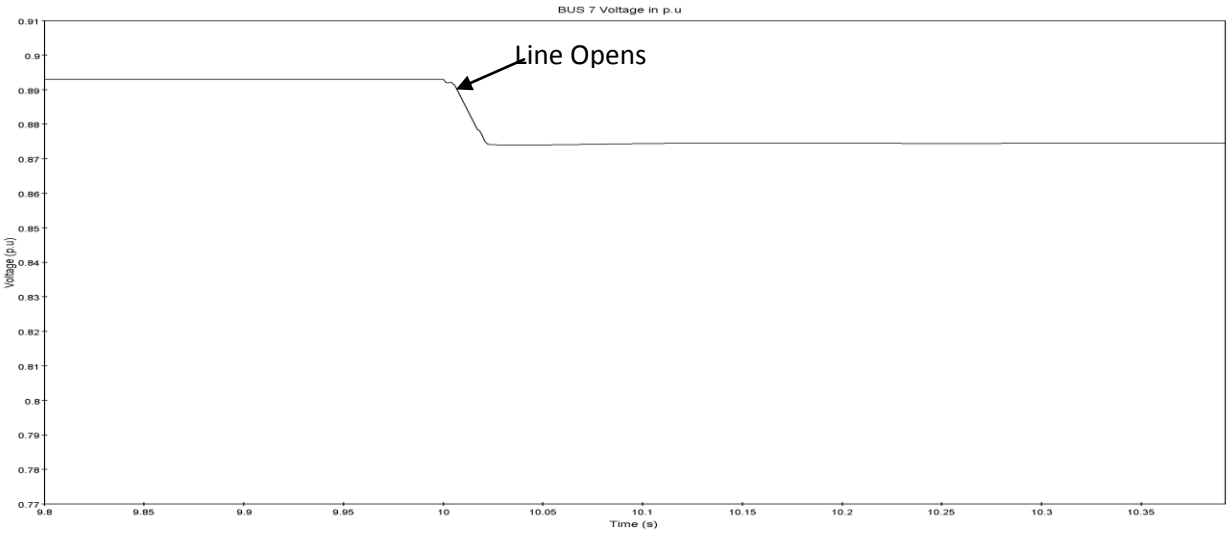

Figure 5.24 Zoomed in Figure 5.23

Figure 5.25 represents Bus 7 voltage for stable test case 1 of Table 5.2. The transmission line was disconnected at 10 seconds and voltage settled around 15 seconds. Figure 5.26 is zoomed in figure of Figure 5.25 around 10 seconds where the transmission line was disconnected.

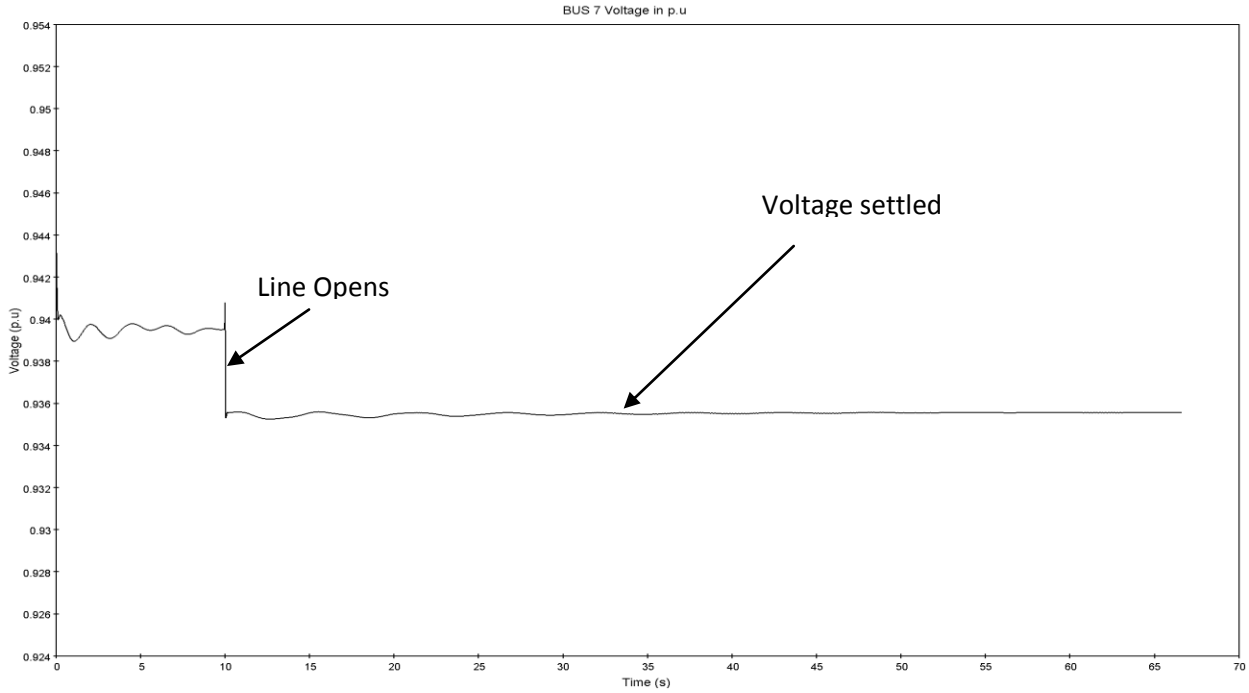

Figure 5.25 Bus 7 voltage for stable Test case 1

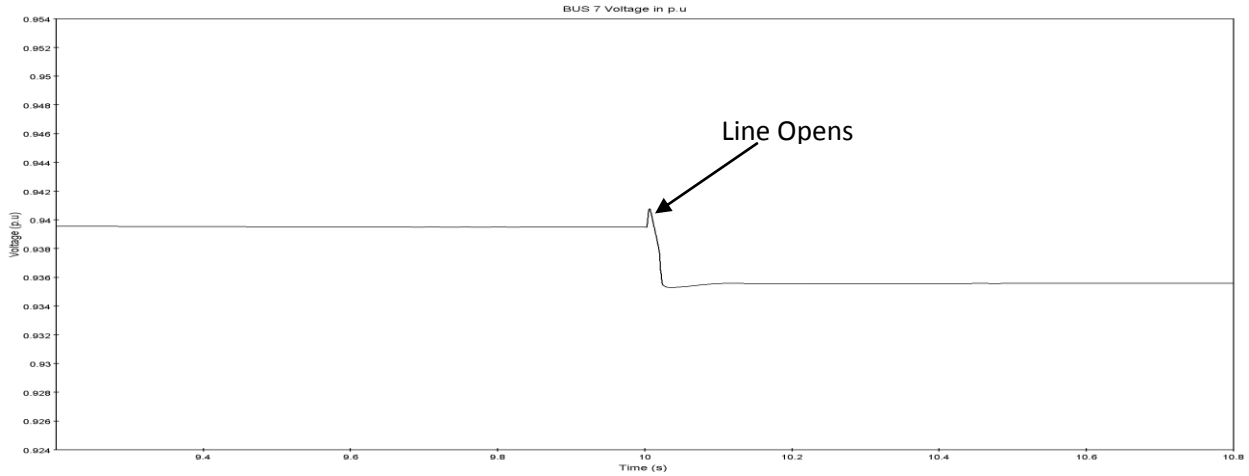

Figure 5.26 Zoomed in Figure 5.25

Figure 5.27 represents Bus 7 voltage for unstable test case 2 of Table 5.2. The transmission line was disconnected at 10 seconds, ULTCs operated with some time delay to restore voltage to precontingency value and at last voltage collapsed around 110 seconds. Figure 5.28 is zoomed in figure of Figure 5.27 around 10 seconds where the transmission line was disconnected.

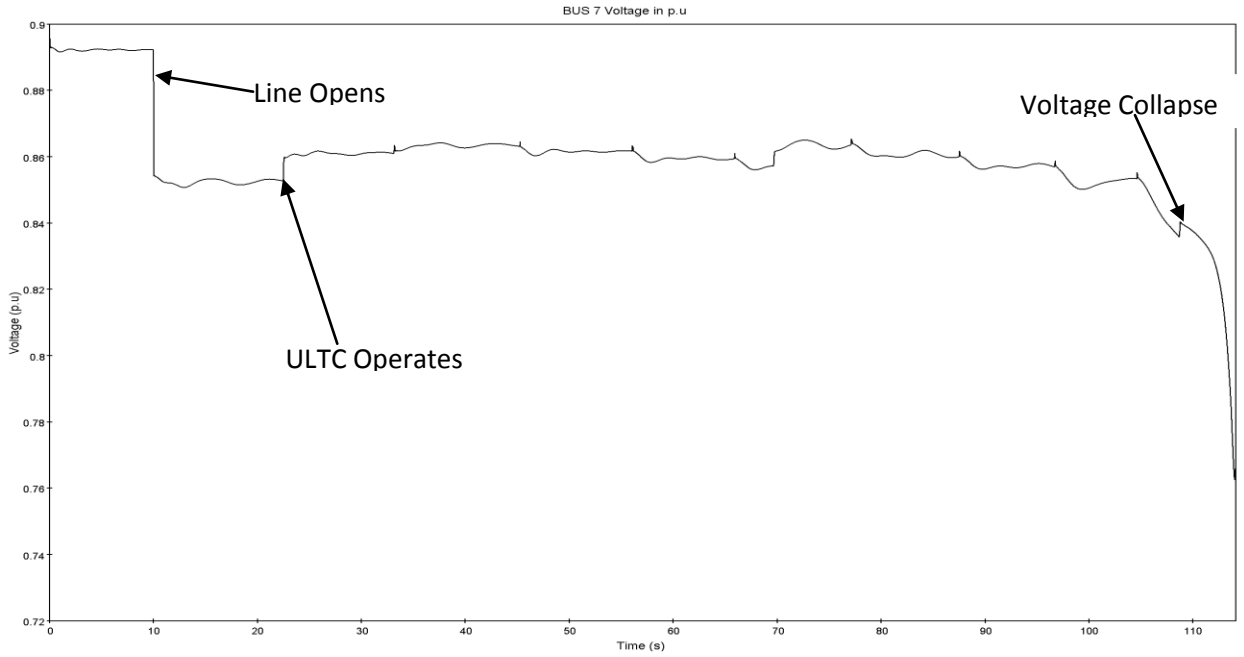

Figure 5.27 Bus 7 voltage for unstable Test case 2

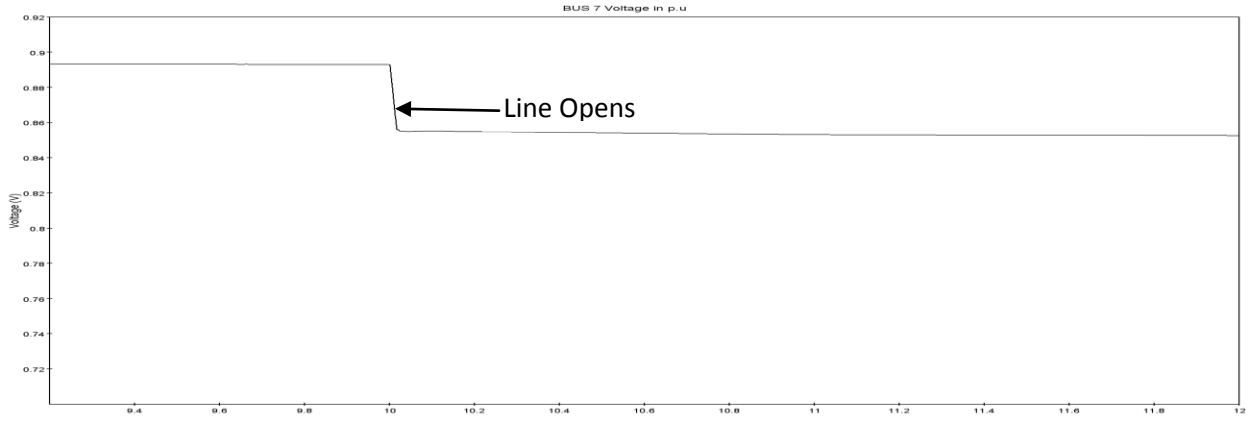

Figure 5.28 Zoomed in Figure 5.27

Figure 5.29 represents Bus 7 voltage for stable test case 3 of Table 5.2. The transmission line was disconnected at 10 seconds, ULTCs operated with some time delay to restore voltage to precontingency value and at last voltage collapsed around 35 seconds. Figure 5.30 is zoomed in figure of Figure 5.29 around 10 seconds where the transmission line was disconnected.

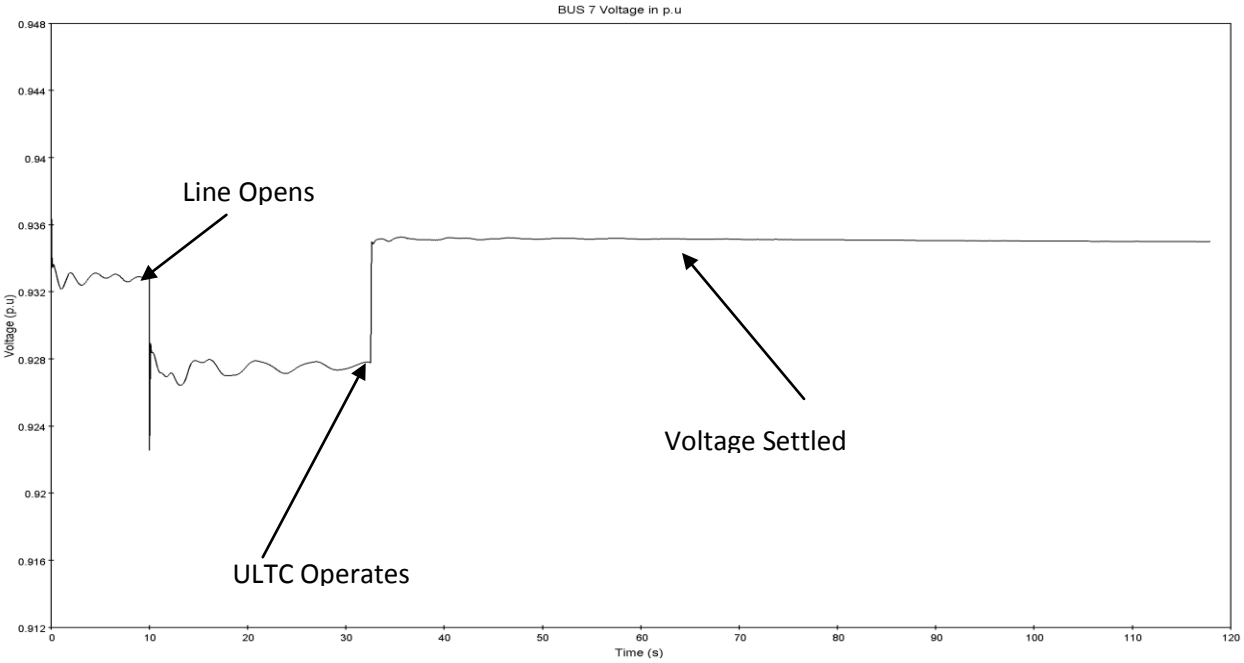

Figure 5.29 Bus 7 voltage for stable Test case 3

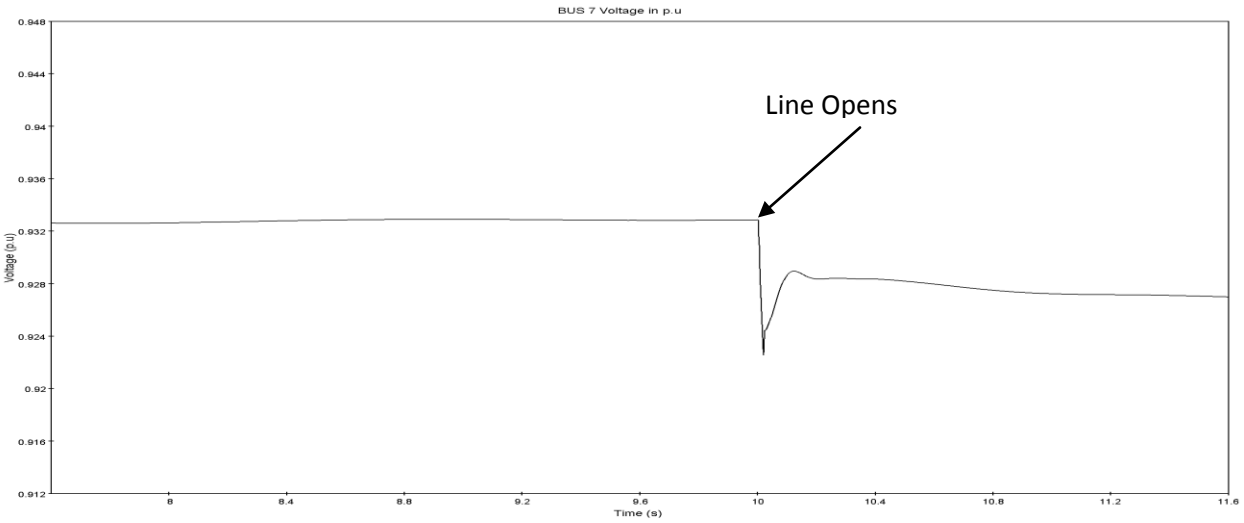

Figure 5.30 Zoomed in Figure 5.29

Figure 5.31 represents Bus 7 voltage for unstable test case 4 of Table 5.2. The transmission line was disconnected at 10 seconds, ULTCs operated with some time delay to restore voltage to precontingency value and at last voltage collapsed around 48 seconds. Figure 5.32 is zoomed in figure of Figure 5.31 around 10 seconds where the transmission line was disconnected.

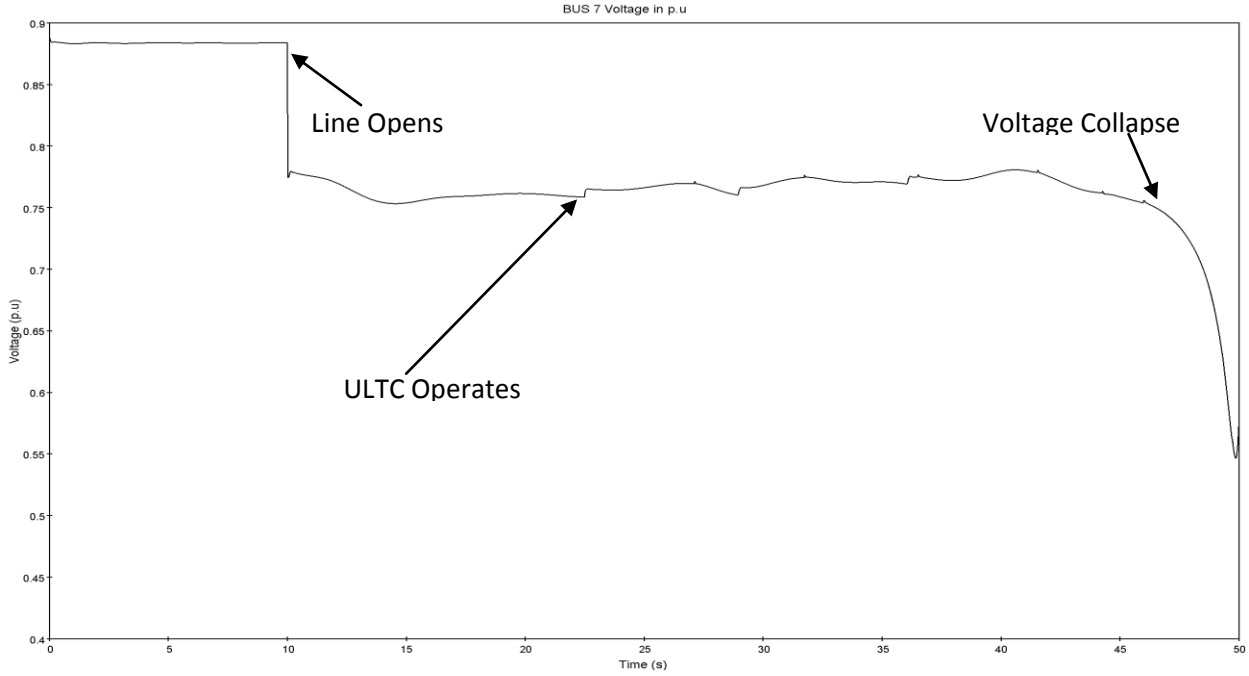

Figure 5.31 Bus 7 voltage for unstable Test case 4

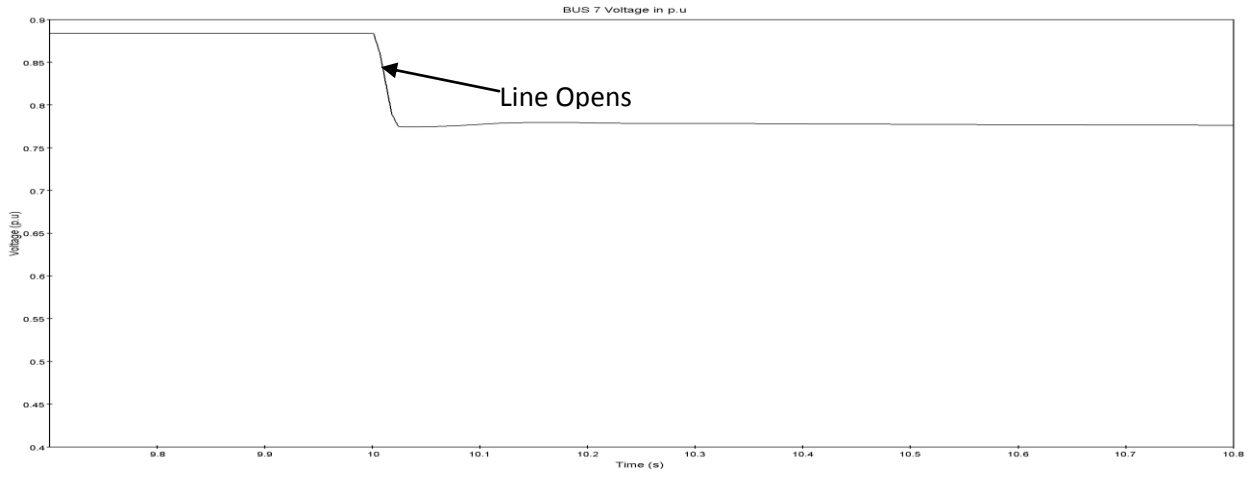

Figure 5.32 Zoomed in Figure 5.31

The trained regularized least-squares classification algorithm using the 10 transient simulation cases of 15 seconds duration were used to predict the voltage stability from the transient stability of the 4 other transient simulation test cases. All these 14 cases simulated in EMTP software were shown in Figure 5.5 to Figure 5.32. After comparing the results from the trained algorithm it is proved that the algorithm is well trained and is 100% accurate in predicting voltage collapse from transient stability.

Table 5.3 Observed Stability from EMTP vs Predicted stability from RLSC

Case	**Observed Stability from EMTP**	**RLSC Predicted Stability**
Test 1	Stable	Stable
Test 2	Unstable	Unstable
Test 3	Stable	Stable
Test 4	Unstable	Unstable

Table 5.3 concludes that the RLSC accurately predicted the voltage stability for all four simulated test cases.

Chapter 6

Summary and Future Work

6.1 Summary

This thesis presented a technique which can detect signs and patterns of power system dynamic behaviors that will drive to voltage collapse in the near future was developed. This method has been proved 100% accurate by applying it on an equivalent IEEE 39 Bus test system in determining voltage instability ahead of time before it is going to happen. This thesis has been concluded that it can predict voltage collapse long before it happens in less than 10 seconds after the transients occurred because of faults on the system or a contingency which involves dynamics of the system. This method is accurate as compared with steady state analysis or snapshot analysis cannot give accurate result because this solution does not consider system dynamics.

A historical review on voltage stability analysis methods have been given in this thesis report. Especially static methods of voltage stability analysis and dynamic methods of voltage stability analysis are compared and advantages and disadvantages have been discussed. Some case studies were included on the major blackouts occurred throughout the world. The main reasons for the blackouts were given in the case studies.

The concepts, definitions and methods required to study the voltage stability and transient stability were presented. Unification of voltage stability and rotor angle stability was given in this report. This unification theory confirms that prediction of voltage stability ahead can be achieved from the transient stability. The proposed technique will analyze the transients occurred

when a contingency or a fault appears in the system, will predict the voltage stability from those transients. This means the proposed technique can predict the voltage collapse before it is going to happen by analyzing the transient behavior of the system for contingencies and faults. To predict the voltage collapse this research used pattern recognition techniques. Regularized least squares classification (RLSC) analysis was used to do the binary classification problems to distinguish voltage stable cases from voltage unstable cases.

The tools and softwares needed to do transient simulation cases on the test system were presented. A small introduction to Hypersim environment and EMTP software have been given in this report. The in build libraries and models of Hypersim and EMTP used in this research were explained with the block diagrams.

The IEEE 39 Bus test system data used to test the proposed technique in predicting voltage instability was given. This data has been converted in such a way that transient simulators can take that data as inputs to do transient simulations. This research included all kinds of dynamics in to the test system by assuming some of the none existing data for IEEE 39 Bus test system.

EMTP was chosen as the main tool to do transient simulations on the IEEE 39 bus test system. A small area has been chosen from the test system to do the simulations, applied different loading conditions and different contingencies to test the proposed technique in identifying voltage instability. Total 10 cases of 15 seconds duration were simulated on the chosen area and trained the RLSC algorithm using those ten cases to predict the voltage instability. 4 other test cases of 15 seconds duration were simulated on the same area and given

these cases as test cases to trained RLSC algorithm and it predicted the voltage instability accurately.

Future Work

The next step is to apply this proposed technique to real-size Entergy's 750 bus system to predict voltage instability ahead of time. This real-size system is going to be build in EMTP and will include all the dynamics to replicate the real Entergy's system. Different scenarios will be simulated on the whole system and will come up with a good training set for the pattern recognition technique which can cover all kinds of contingencies and faults. These simulated cases will be used to predict the voltage instability ahead of time. Then these simulation cases will be given as inputs to the different kinds of pattern recognition techniques. The main goal is to come up with a good pattern recognition technique which is 100% accurate and efficient for the Entergy's system in predicting voltage collapse. Our next goal is to come up with a mathematical model to determine voltage collapse from transient stability to conclude that prediction of voltage collapse will be possible from the transient stability before the voltage collapse going to occur.

Bibliography

[1] Kundur. P. Power system voltage Stability and Control. *Mc-Graw Hill*, New York, 1994.

[2] Tamura. Y. Relationship between voltage instability and multiple load flow solutions in electric power system. *IEEE Trans. on PAS*, Vol. PAS-102, May 1983, pp. 1115-1125

[3] Galiana. F. D. Load flow feasibility and the voltage collapse problem. *IEEE Proceedings of 23th Conference on Control and Decision*, Las Vegas, Dec. 1984, pp. 485-487

[4] Carpentier. J. et al. Voltage collapse proximity indications computed from an optimal power flow. *Proc. Of Computation Conference*, Helsinki, Finland, September 1984, pp. 671-678

[5] Brucoli. M. et al. A generalized approach to the analysis of voltage stability in electric power systems. *Electric Power Systems Research*, Vol. 9, 1985, pp. 49- 62

[6] Van Cutsem. T, Vournas, C. Voltage stability of electric power systems. *Kluwer academic publishers*, Boston, USA, 1998, 378 p.

[7] Taylor. C. W. Power system voltage stability. *McGraw-Hill*, New York, USA, 1994, 273p

[8] Lee. B. H, Lee. K. Y. A study on voltage collapse mechanism in electric power systems. *IEEE Trans. Power Systems*, Vol. 6, August 1991, pp. 966-974

[9] Löf. P-A, Andersson. G, Hill. D. J. Voltage stability indices for stressed power systems. *IEEE Trans. Power Systems*, Vol. 8, February 1993, pp. 326-335

[10] Löf. P-A, Andersson. G, Hill. D. J. Voltage dependent reactive power limits for voltage stability studies. *IEEE Trans. Power Systems*, Vol. 10, February 1995, pp. 220-228

[11] Gao. B, Morison. G. K, Kundur. P. Voltage stability evaluation using modal analysis. *IEEE Trans. Power Systems*, Vol. 7, November 1992, pp. 1529-1542

[12] Guckenheimer. J, Towards a global theory of singularly perturbed dynamical systems. *Progress in Nonlinear Differential Equations and Their Applications*, 19, 1996, pp.214-225

[13] Kwanty. H. G, Pasrija. A. K, Bahar. L.Y. Loss of steady state Stbility and voltage collapse in electric power systems. *Proceedings of 24th conference on Decision and Control*. Ft. Lauderdale, Fl, Dec 1985.

[14] Van Cutsem. T. et.al. A comprehensive analysis of mid-term voltage stability. *IEEE Transactions on Power Systems*, Vol.10, No. 3, August 1995, pp. 1173-1182

[15] Ajjarapu. V, Christy. C. The continuation power flow: A tool for steady state voltage stability analysis. *IEEE Trans. on Power Systems*, Vol. 7, No.1, February 1992, pp. 416-243

[16] Morison. G. K, Gao. B, Kundar. P. Voltage stability analysis using static anddynamic approaches. *IEEE Tran. on Power Systems*, Vol. 8, No.3, August 1993, pp. 1159-1171

[17] Begovic. M. M, Phadke. A. G. Control of voltage stability using sensitivity analysis. *IEEE Transactions on Power Systems*, Vol.7, No.1, February 1992, pp. 114-123.

[18] DeMarco. C. L, Overbye. T. J. Improved techniques for power systen voltage stability assessment using energy methods. *IEEE Transactions on Power Systems*, Vol.6, No.4, November 1991, pp. 1446-1452.

[19] Huang. G, Zhu. T. A new method to find the voltage collapse point. *Proc. of Power Engineering Society Winter Meeting IEEE*, Vol. 2, Edmonton, Canada, July 1999, pp1324-1329

[20] Rastgoufard. P, Bian. J. Power system voltage stability and security assesment. *Third Biennial Symposium on Induxtrial Electric Power Applications*, New Orleans, LA, Nov 12-13, 1992, pp178-183.

[21]C. Sharma, Marcus G. Determination of Power Sytem Voltage Stability Using Modal Analysis. *POWERENG 2007*, April 2007, Portugal.

[22]Li-Jun. C, Istavan. E. Power System Static Voltage stability analysis considering all Active and Reactive Power Controls- singular Value approach. *POWERTECH 2007*.

[23] Zeng. Y. G, Berizzi. A, Marannino. P. Voltage stability analysis considering dynamic load model. *Proceedings of the 4th International Conference on Advances in Power System Control, Operation and Management*, APSCOM-97, Hong Kong, November 1997.

[24] Wison Xu, Yakout. M. Voltage stability analysis using generic dynamic load models. *IEEE Transactions on Power Systems*. Vol. 9, No. 1, February 1994.

[25] Haque. M. H, Pothula. U. M. R. Evaluation of Dynamic Voltage Stability of a Power System. *POWERCON 2004*, Singapore.

[26] Liu. C. C. Characterization of a voltage collapse mechanism due to the effect of on-load tap changers. *Proc, 1986 IEEE International Symposium on Circuits and systems*, Vol.3, May 1986, pp. 1028-1030.

[27] Liu. C. C, KHOI. T. VU. Analysis of Tap-Changer Dynamics and Construction of voltage Stability Regions. *IEEE Transaction on circuits and systems*, Vol. 36, no. 4, April 1989.

[29] Sekine. Y, Ohtsuki. H, Cascaded voltage collapse. *IEEE Trans. Power Systems*, Vol. 5, no. 1, February 1990, pp. 250-256.

[30] Wong. C .S .M, Rastgoufard. P, Mader. D. Voltage Stability Studies Using Real-Time Simulation Computing. *System Theory*, 2008. SSST 2008. 40th Southeastern Symposium on, March 2008, pp. 410 – 414.

[31] Atputharajah. A, Tapan. K. S, Power system blackouts- Literature review. *Fourth International Conference on Industrial and Information Systems*, ICIIS 2009, 28 - 31 December 2009, Sri Lanka.

[32] Lee. C. W, John. A. C, Lawrence 1 Connor., Charles. R. R, Carl. E. B. Prevention ofpower failures. *Volume 1- Report of the commission submitted to the President by Federal Power Commission*,July 1967.

[33] Ilic. M, Chow. J. H, Galiana. F. D, Shahidehpour. M, Thomas. R. J, Wu. F. F. Special Issue on Power Technology and Policy: Forty Years after the 1965 Blackout. *Proceedings of the IEEE*, Vol. 93, no. 11, November 2005.

[34] Blackout on August 14, 2003 Final Report February by New York Independent System Operator. Feb 2005.

[35] Chunyan. L, Yuanzhang. S, Xiangyi. C. Recommendations to improve power system security: Lessons learned from the Europe blackout on Nov 4th 2006. UPEC-2007.

[36] Wong. C. S. M, Leevongwat. I, Rastgoufard. P. Angle and magnitude stability using Real-Time Simulation. *Transmission and Distribution Conference and Exposition, 2008. T&D. IEEE/PES*, April 2008, pp. 1 - 4 .

[38] Wong. C. S. M. Unification of Angle and Magnitude Stability to InvestigateVoltage Stability of Large-Scale Power System. *PhD thesis, Dept. ofElectrical Engineering and Computer Science*, Tulane University, 2007.

[39] Athay. T, Sherkat. V. R, Podmore. R, Virmani. R, Puech. C. Transient Energy Analysis. *Final report of U.S department of energy Contract No. Ex-76-C-012076*, Prepared by systems control, Inc., June 1979.

[40] Chi-Keug. T, Evaluation of the direct method for power system transient stability analysis. *M.Eng degree thesis*, University of Toronto, August 1984.

[41] Duda. R. O, Hart. P. E, Stork. D. G. Pattern Classification. *John Wiley & Sons,Inc*., 2nd ed. 2000, 680p.

[42] Poggio. T, Smale. S. The mathematics of learning: Dealing with data. *Amer. Math. Soc. Notice*, Vol.50 (5), 2003, pp. 537-544

[43] Rifkin. R. M. Everything Old is New Age: A fresh look at historical Approaches to Machine Learning. *PhD thesis*, Massachusetts Institute of Technology, 2002

[44] Hypersim Software version 9.1 Reference Guide Manual. TransEnergy Technologies.

[45] K.R. Padiyar. Power System Dynamics: Stability & Control. B.S. Publications, India, 2002

[46] Gupta. J. B. Theory and Electrical performance of Electrical Machines. *S. Kataria and sons*.

[47] Bian. J, Modal analysis of large scale power systems voltage stability and Voltage collapse. *Ph. D. Dissertation*, Tulane University, December 1992.

[48] Bernhard. S, Ralf. H, Alex. S. A generalized representar theorem. *14th Annual conference on computational learning theory*, Pages 416-426, 2001.

[49] Grace. W. Spline models for observational data. *volume 59 of CBMS-NSF Regional conference series in applied mathematics*. Society for Industrial & Applied Mathematics, 1990.

Vita

The author was born in 1986, in India. He completed his bachelors of technology degree in Electrical and Electronics Engineering from JNTU, Hyderabad India in 2007 with distinction. He finished his Masters in Electrical Engineering from the University of New Orleans in December 2010 with a cumulative GPA of 3.70. He worked as an intern in summer 2009 at Entergy Services Inc. Now the author is moving towards his PhD degree at University of New Orleans and is working as a Research Assistant under Prof. Dr. Parviz Rastgoufard. His areas of interests are real time simulation studies, real time testing, and real time simulation modeling.